

# *Biochar modification to enhance sorption of inorganics from water*

Article

Accepted Version

Creative Commons: Attribution-Noncommercial-No Derivative Works 4.0

Sizmur, T. ORCID: <https://orcid.org/0000-0001-9835-7195>, Fresno, T., Akgül, G., Frost, H. and Moreno-Jiménez, E. (2017) Biochar modification to enhance sorption of inorganics from water. *Bioresource Technology*, 246. pp. 34-47. ISSN 0960-8524 doi: <https://doi.org/10.1016/j.biortech.2017.07.082> Available at <https://centaur.reading.ac.uk/71915/>

It is advisable to refer to the publisher's version if you intend to cite from the work. See [Guidance on citing](#).

Published version at: <https://doi.org/10.1016/j.biortech.2017.07.082>

To link to this article DOI: <http://dx.doi.org/10.1016/j.biortech.2017.07.082>

Publisher: Elsevier

All outputs in CentAUR are protected by Intellectual Property Rights law, including copyright law. Copyright and IPR is retained by the creators or other copyright holders. Terms and conditions for use of this material are defined in the [End User Agreement](#).

[www.reading.ac.uk/centaur](http://www.reading.ac.uk/centaur)

**CentAUR**

Central Archive at the University of Reading

Reading's research outputs online



# **Biochar modification to enhance sorption of inorganics from water**

Tom Sizmur<sup>1</sup>, Teresa Fresno<sup>2</sup>, Gökçen Akgül<sup>3</sup>, Harrison Frost<sup>1</sup>, Eduardo Moreno Jiménez<sup>2\*</sup>

<sup>1</sup>*Department of Geography and Environmental Science, University of Reading, Reading, RG6 6DW, UK*

<sup>2</sup>*Department of Agricultural and Food Chemistry, Faculty of Sciences, Universidad Autonoma de Madrid, 28049, Madrid,*

*Spain*

<sup>3</sup>*Recep Tayyip Erdogan University, Engineering Faculty, Department of Energy Systems Engineering, 53100, Rize, Turkey*

\*Corresponding author: Eduardo Moreno Jiménez, Department of Agricultural and Food Chemistry, Faculty of Sciences, Universidad Autonoma de Madrid, 28049, Madrid, Spain. Phone: +34914978470; email: [eduardo.moreno@uam.es](mailto:eduardo.moreno@uam.es)

## **Abstract**

Biochar can be used as a sorbent to remove inorganic pollutants from water but the efficiency of sorption can be improved by activation or modification. This review evaluates various methods to increase the sorption efficiency of biochar including activation with steam, acids and bases and the production of biochar-based composites with metal oxides, carbonaceous materials, clays, organic compounds, and biofilms. We describe the approaches, and explain how each modification alters the sorption capacity. Physical and chemical activation enhances the surface area or functionality of biochar, whereas modification to produce biochar-based composites uses the biochar as a scaffold to embed new materials to create surfaces with novel surface properties upon which inorganic pollutants can sorb. Many of these approaches enhanced the retention of a wide range of inorganic pollutants in waters, but here we provide a comparative assessment for  $\text{Cd}^{2+}$ ,  $\text{Cu}^{2+}$ ,  $\text{Hg}^{2+}$ ,  $\text{Pb}^{2+}$ ,  $\text{Zn}^{2+}$ ,  $\text{NH}_4^+$ ,  $\text{NO}_3^-$ ,  $\text{PO}_4^{3-}$ ,  $\text{CrO}_4^{2-}$  and  $\text{AsO}_4^{3-}$ .

**Keywords: Modification, sorption, inorganic, pollution, activation**

## 1. Introduction

Biochar is produced by heating organic materials in the partial or total absence of oxygen (pyrolysis). The objective of biochar production is usually to generate energy or to reduce the mass or volume of waste materials. However, considerable interest has been paid to optimising the pyrolysis conditions to improve the yield (Tripathi et al., 2016) and properties (Mukherjee et al., 2011) of the resulting biochar. Biochar is resistant to degradation, has a high surface area and a considerable negative charge (Sizmur et al., 2016). It has therefore been proposed as a sustainable means to remove positively charged ions (e.g.  $\text{Cd}^{2+}$ ,  $\text{Cu}^{2+}$ ,  $\text{Pb}^{2+}$ ,  $\text{Zn}^{2+}$ ) and polar organic molecules (e.g. phenolics, halogenated compounds, solvents) from water by ion exchange, electrostatic attraction, physical sorption and precipitation (Tan et al., 2015).

There are several methodologies by which the properties of biochar can be chemically, physically or biologically modified by treating the feedstock or, more commonly, the resulting biochar (Rajapaksha et al., 2016). These methodologies include treatments with steam, acids, bases, metal oxides, carbonaceous materials, clay minerals, organic compounds, and biofilms. The objectives of these treatments are broadly to either, (i) increase the surface area of the biochar, (ii) modify or enhance the surface properties of the biochar, or (iii) use the surface as a platform to embed another material (or organism) with beneficial surface properties. The tools available to modify biochars increase the breadth of chemical pollutants which can be removed from water using biochar.

This review will provide an introduction to common inorganic pollutants, describe the surface properties of unmodified biochar, introduce the various modification approaches, explain how the pyrolysis process and the modifications alter the surface properties of biochar, and demonstrate how these modifications enhance the removal of inorganic contaminants from aqueous solutions.

## 2. Common inorganic pollutants in water

The prevention and remediation of freshwater pollution is one of the greatest global challenges facing humanity in the 21<sup>st</sup> century (Dudgeon et al., 2006). Anthropogenic disruption of biogeochemical cycling of elements has increased the concentrations, or changed the chemical form, of several elements in terrestrial ground and surface waters. The inorganic contaminants of primary concern are classified by their chemical behavior and discussed below. Efficient, sustainable, and cost-effective remediation strategies for these elements are urgently required.

Potentially toxic elements, such as As, Cd, Cr, Cu, Hg, Pb and Zn are often present discharges from mining and smelting, sewage treatment, road runoff and the manufacture of batteries, pigments and dyes, electronics and alloys (Moore & Ramamoorthy, 2012). In sufficient concentrations, these elements can cause ecotoxicological effects to freshwater ecology and can bioaccumulate through food webs resulting in chronic toxicity to higher trophic levels, including humans. Most of these elements (Cd, Cu, Hg, Pb, and Zn) occur primarily in the environment as divalent cations. Cd and Zn have a larger radius and thus a lower charge-to-radius ratio and lower ionic potential than Cu, Hg and Pb. For this reason, Cu, Hg and Pb more readily form bonds with functional groups on surfaces and are thus less mobile than Cd and Zn.

Concentrations of nutrients ( $\text{NH}_4^+$ ,  $\text{NO}_3^-$  and  $\text{PO}_4^{3-}$ ) are elevated in surface and ground waters globally, largely due to sewage effluent and inefficient application of agricultural fertilizers, (Mueller & Helsel, 1996). The elevated nutrient status of freshwater discharges to oceans causes ecological damage in estuaries and coastal zones by promoting harmful algal blooms, and reducing dissolved oxygen concentrations, resulting hypoxic 'dead zones' (Conley et al., 2009).

While  $\text{NH}_4^+$  is positively charged and is attracted to the negatively charged surfaces, it has a much lower charge-to-radius ratio than the metal cations discussed above.  $\text{NH}_4^+$  thus behaves similarly to alkali metal cations (e.g.  $\text{Na}^+$ ,  $\text{K}^+$ ) and so does not form as stable bonds with surfaces as the divalent metal cations. Unlike  $\text{NH}_4^+$ ,  $\text{NO}_3^-$  and  $\text{PO}_4^{3-}$  are oxyanions with contrasting behavior to each other. Both are negatively charged and therefore attracted to positively charged surfaces but  $\text{NO}_3^-$  is much more mobile than  $\text{PO}_4^{3-}$ , which readily binds to colloids in water.

As and Cr are redox sensitive elements that exhibit contrasting changes to mobility and toxicity in response to changes in redox conditions. Inorganic As can be found in the environment as pentavalent arsenate, As(V), or as trivalent arsenite, As(III). Arsenate ( $\text{AsO}_4^{3-}$ ) is found in aerobic environments, and arsenite ( $\text{AsO}_3^{3-}$ ), which is more toxic to humans, is more mobile, and occurs in anaerobic conditions, including groundwater (Moore & Ramamoorthy, 2012). The use of naturally occurring As contaminated groundwater as drinking water and to irrigate rice paddies has resulted in widespread poisoning of human populations, especially in Bangladesh. Cr can be found as trivalent Cr(III) and hexavalent Cr(VI). In contrast to As, the reduced species, Cr(III) is considered a beneficial element in humans as it enhances insulin production, whereas Cr(VI), usually present as chromate ( $\text{CrO}_4^{2-}$ ) or dichromate ( $\text{Cr}_2\text{O}_7^{2-}$ ) is a strong oxidising agent, is carcinogenic, and is more mobile and much more toxic than Cr(III) (Kotaś & Stasicka, 2000). Chromium most notoriously contaminates surface waters due to discharge of tannery effluent .

To reduce the concentrations of these inorganic contaminants of concern in aquatic ecosystems it is essential to treat point source discharges of agricultural, domestic and industrial wastewater before disposal into the freshwater environment. Current wastewater treatment technologies to remove inorganic contaminants are costly, energy intensive, and require disposal of resulting toxic waste (Shannon et al., 2008). These limitations of the

currently available technologies provide a demand for an efficient, selective, cost-effective adsorbent material. The modification of biochar could provide the versatile, low cost and sustainable solution to point source pollution of freshwater with inorganic pollutants.

### **3. How biochar properties influence the sorption of inorganic pollutants from aqueous solutions**

Biochar can be used as a sorbent to remove pollutants from water and may be removed from solution when saturated, treated appropriately and replaced with new or recycled biochar. There are several mechanisms responsible for the high sorption capacity of biochar for specific pollutants.

Biochars have a high surface area due to a large distribution of micro or mesopores. The greater the number of micropores, the greater the surface area of the biochar and the more surface sites upon which pollutants can adsorb. Several authors have observed a relationship between pollutant adsorption capacities and biochar surface area (Kim et al., 2013; Tan et al., 2015).

Surface functionality also affects biochar sorption capacity (Fletcher et al., 2014; Niu et al., 2017). Sorption of inorganic pollutants by biochar is a result of (i) stoichiometric ionic exchange, (ii) electrostatic attraction, or (iii) surface precipitation (Beesley et al., 2015; Gomez-Eyles et al., 2013; Sizmur et al., 2016).

(i) Chemical sorption occurs due to ion exchange with the abundant functional groups on the carbonaceous surface of biochar, such as carboxylic, hydroxylic or phenolic groups (Lee et al., 2010; Liang et al., 2006). These groups confer cation exchange capacity (CEC) to biochar depending on feedstock and pyrolysis temperature, with a peak of CEC at around 350-400 °C (Gomez-Eyles et al., 2013), probably due to the loss of oxygenated functional groups above this temperature (Lee et al., 2010). Chemical sorption of cations relies on releases of protons and base cations (Na, K, Ca or Mg) from the biochar (Uchimiya et al., 2010). Since chemical

sorption is stoichiometric, sorption efficiency is pH dependent and thus dictated by the pH of the medium.

(ii) Physical (electrostatic) sorption occurs between positively charged ions in water and the delocalised cloud of electrons associated with aromatic groups on the surface of carbonaceous biochars, creating cation- $\pi$  interactions with the C=C aromatic bonds (Harvey et al., 2011). Unlike chemical sorption, physical adsorption does not require stoichiometric release of cations or protons from the biochar.

(iii) Precipitation (or co-precipitation) of inorganic pollutants (particularly metal cations) with insoluble salts occurs on the surface of biochars with a high mineral ash content. For example, precipitation of Pb has been demonstrated on the surface of phosphate rich biochars derived from manures (Cao et al., 2009). Biochar may also raise the pH of the solution (depending on its starting pH), leading to the precipitation of metal (hydr)oxides, which are generally sparingly soluble.

Surface area and functionality can be manipulated by the modification of biochar to enhance sorption capacities for specific pollutants. Modifications often have the objective of increasing the anion sorption capacity while activation usually increases the metal cation sorption capacity of biochars. However, considerable differences in the surface area and functionality of biochars can result from altering the pyrolysis temperature.

#### **4. Effect of pyrolysis temperature on biochar properties and sorption capacity**

Although modifications of biochars (post-pyrolysis) or their feedstocks (pre-pyrolysis) can alter their physico-chemical properties, pyrolysis conditions can also affect the biochar structure and composition and thus its metal sorption capacity (Figure 1). Pyrolysis temperature influences the adsorption characteristics of biochar by changing the surface area, surface functionality, pore distribution and mineral concentration of biochar (Ahmad et al.,



2012; Chen et al., 2014; Jung et al., 2016b; Kim et al., 2012). It is important to produce biochar at optimum pyrolysis temperatures to maximise inorganic contaminant adsorption.

The development of microstructure and an increase in the surface area of biochar upon increasing pyrolysis temperature has been widely observed, regardless of the feedstock used (Cantrell et al., 2012; Fletcher et al., 2014; Uchimiya et al., 2010). Fletcher et al. (2014) observed an opening of the internal structure when the pyrolysis temperature of willow biochar was  $\geq 450$  °C. At higher temperature ( $\geq 550$  °C), the width of mesopores increased and new micropores were created. However, Jung et al. (2016b) found a decrease in total pore volume, surface area and phosphate sorption capacity of a biochar produced from a marine macroalgae when pyrolysis temperature increased to 600 and 800 °C, likely due to blockage and collapse of the pore structures (Paethanom & Yoshikawa, 2012) by melting of the material during pyrolysis.

Biochars produced at higher temperatures often contain greater amounts of C fixed in the biochar structure (i.e. higher C content) as a result of greater loss of volatile matter at high pyrolysis temperatures (Cantrell et al., 2012; Kim et al., 2012). Increasing pyrolysis temperatures also increases the aromaticity and decreases the polarity of the biochar, so the biochar surface becomes less hydrophilic. Lower O and H contents have been reported when increasing pyrolysis temperature due to loss of surface functional groups. The decrease in oxygen-containing functional groups can affect the metals sorption capacity of biochars, as observed by Ding et al. (2014), who found higher Pb adsorption capacity of biochar when produced at lower temperature. The authors suggest that for lower temperature biochars, oxygen-containing functional groups were responsible for Pb sorption, whereas for high temperature biochars, Pb sorption was dominated by intraparticle diffusion and was thus affected by the abundant pores.

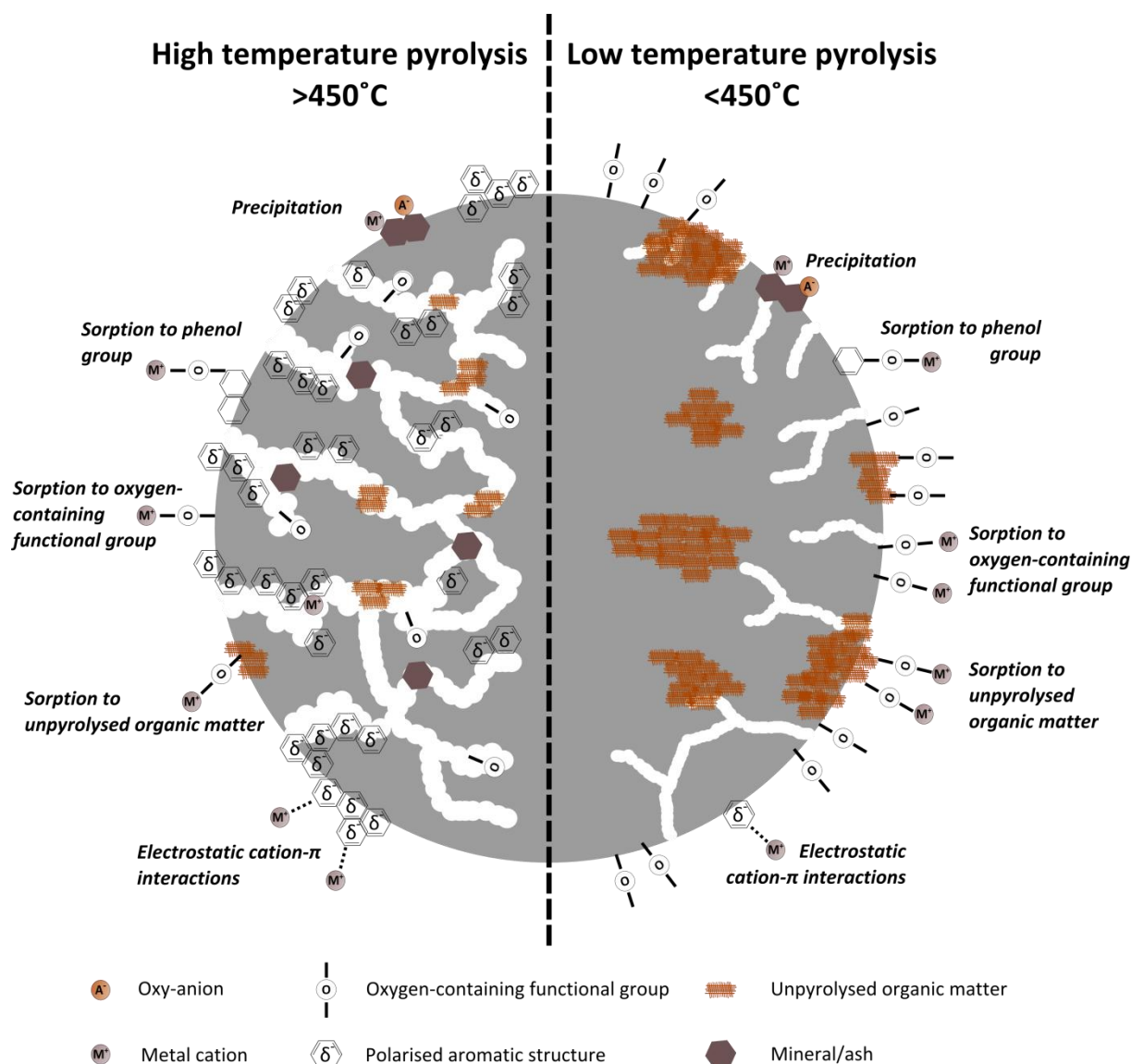


**Figure 1. Conceptual model identifying the mechanisms of metal cation (e.g. Cd<sup>2+</sup>, Cu<sup>2+</sup>, Hg<sup>2+</sup>, Pb<sup>2+</sup>, Zn<sup>2+</sup>) and oxyanion (e.g. PO<sub>4</sub><sup>3-</sup>, AsO<sub>4</sub><sup>3-</sup>) sorption to biochar pyrolysed at high temperature (>450°C) and low temperature (<450°C). High temperature biochar has a higher surface area, pores previously blocked by unpyrolysed organic matter are unblocked, and there are more aromatic groups and less oxygen containing functional groups on the biochar surface.**

The yield of biochar production decreases as pyrolysis temperature increases, generally by about 10% for every temperature increase of 100 °C (Chen et al., 2014; Fletcher et al., 2014). As the pyrolysis temperature increases and the biochar yield decreases, the mineral ash content becomes more concentrated. Consequently, biochars produced at higher pyrolysis temperatures have more total, soluble and exchangeable base cations and carbonates, less

oxygenated functional groups and greater pH (Fletcher et al., 2014; Qian et al., 2013; Yuan et al., 2011). Thus, more alkaline biochar can be produced by increasing the pyrolysis temperature, which can lead to greater precipitation of metal cations (Kim et al., 2013). Chen et al. (2014) reported higher Cd removal from an aqueous solution by biochar produced with a mixture of sewage sludge and pine bark when biochar was produced at higher pyrolysis temperature. The authors suggested that  $\text{Cd}^{2+}$  sorption onto biochar was likely due to surface precipitation with  $\text{Ca}^{2+}$  and thus attributed the higher Cd removal to the enhanced cation exchange capacity in higher temperature-biochar due to concentrated alkaline-earth metals, such as  $\text{Ca}^{2+}$ , in the ash during pyrolysis.

## **5. Methods of modifying Biochar**

Innovative methodologies for modifying biochar have been developed to enhance the adsorption of inorganic pollutants from water. Modifications are performed either pre- or post-pyrolysis of the biochar (or both). Whilst pre-pyrolysis modifications involve the treatment of the biochar feedstock, post-pyrolysis modifications are more common and involve the treatment of biochar after it has already been produced. Figure 2 provides a classification system of the most common modification methods reported in the literature. The physical activation of biochar using steam and chemical activation using acidic and alkaline solutions is usually undertaken post-pyrolysis, although promising results have been reported also when chemical activation is conducted pre-pyrolysis. The production of biochar-based composites, the modification method that has received the most research attention for creating sorbents for remediation of polluted waters, is performed by embedding different materials into the biochar structure pre- or post-pyrolysis. The primary aim of all these modification methods is to enhance the efficacy by which the biochar removes pollutants from water, generally by changing its physical or chemical properties, such as surface area, or surface functionality.

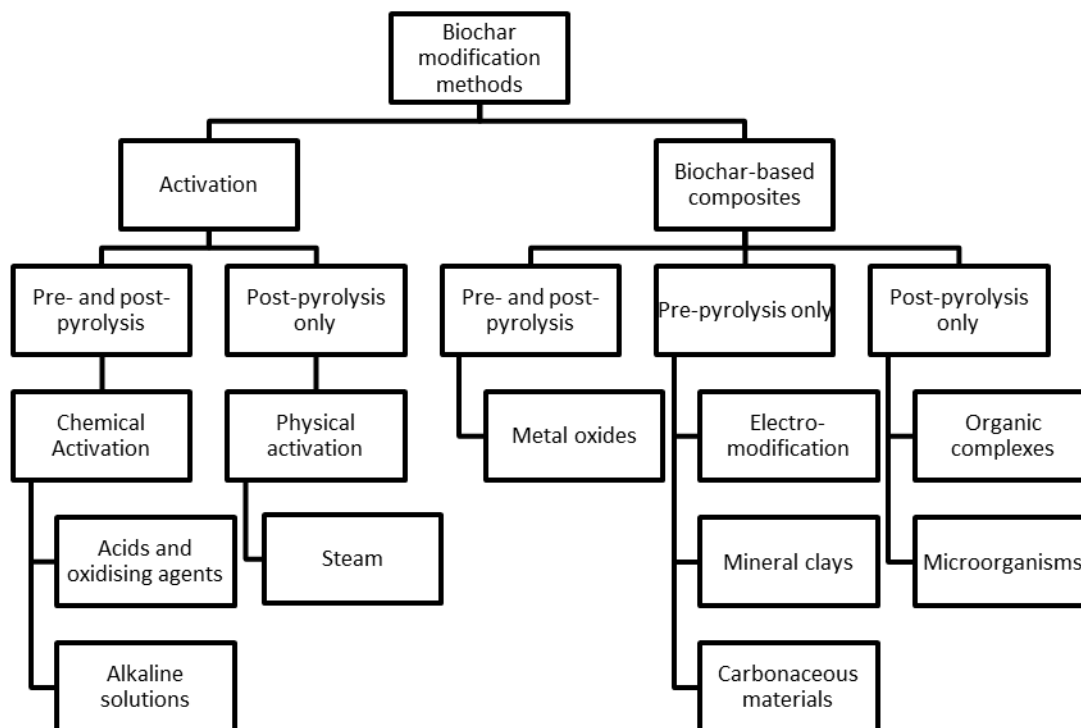


**Figure 2. Chart defining a classification system of biochar modification methods to physically and chemically activate biochars and produce biochar based composites**

The properties of biochar can be altered by physical and chemical activation. While the acid and alkali treatments are the most common chemical activation methods, steam is the primary physical activation method. Biochar-based composites are prepared by impregnation or coating the surface of the biochar with metal oxides (Micháleková-Richveisová et al., 2017), clay minerals (Chen et al., 2017), carbonaceous structures such as graphene oxide (Shang et al., 2016) or carbon nanotubes (Inyang et al., 2015), complex organic compounds, such as chitosan (Zhou et al., 2013) or amino acids (Yang & Jiang, 2014), or inoculation with microorganisms (Frankel et al., 2016). These modification methods are explained in detail in the following sections and their impact on the sorption of selected inorganic pollutants in water are summarised in Table 1.

253 **Table 1. Effect of biochar modifications on common inorganic pollutants in water. The modifications were sorted as Physical**  
 254 **activation with steam (Phy. A. – Steam); Chemical activation with acids or oxidants (Ch. A. - Acids/oxidants) or with bases (Ch. A. -**  
 255 **Acids/oxidants); Biochar-based composites (Comp.) modified with metals (Metals), carbonaceous materials (C materials), electrical**  
 256 **field (Electromodified), organic molecules (Organics) and Biofilms (microorganisms).**

Target pollutant	Type of biochar modification	Treatment / Feedstock	Treatment stage	Effect on metal sorption capacity	References
<b>Cd<sup>2+</sup></b>	Phy. A. - Steam	Steam / Poultry manure)	Post-pyrolysis	+	Lima and Marshall (2005)
	Ch. A. - Bases	KOH / Ipomoea biomass	Post-pyrolysis	+	Goswami et al., (2016)
	Comp. - Metals	Fe / Several feedstocks	Post-pyrolysis	+	Mohan et al., (2014); Trakal et al., (2016)
	Comp. - Organics	Chitosan / Bamboo, hickory wood, sugarcane bagasse	Post-pyrolysis	+	Zhou et al., (2013)
	Comp. - Organics	Chitosan / Peanut hull	Post-pyrolysis	-	Zhou et al., (2013)
<b>Zn<sup>2+</sup></b>	Phy. A. - Steam	Steam / poultry manure	Post-pyrolysis	+	Lima and Marshall (2005)
<b>Cu<sup>2+</sup></b>	Phy. A. - Steam	Steam / Pine sawdust	Post-pyrolysis	=	Lou et al., (2016)
	Phy. A. - Steam	Steam / poultry manure	Post-pyrolysis	+	Lima and Marshall (2005)
	Ch. A. - Acids/oxidants	HNO <sub>3</sub> / Cactus cladodes	Post-pyrolysis	+	Hadjitoffi et al., (2014)
	Ch. A. - Bases	KOH / Fruit peel	Post-pyrolysis	+	Hamid et al., (2014)
	Comp. - Metals	Mn / Corn straw	Post-pyrolysis	+	Song et al., (2014)
	Comp. - Organics	Amino-modification by nitrification and reduction / Commercial sawdust	Post-pyrolysis	+	Yang and Jiang, (2014)
	Comp. - Organics	Chitosan / Bamboo, hickory wood, sugarcane bagasse, peanut hull	Post-pyrolysis	-	Zhou et al., (2013)
<b>Hg<sup>2+</sup></b>	Comp. - C materials	Graphene oxide / Wheat straw	Pre-pyrolysis	+	Tang et al., (2015)
<b>Pb<sup>2+</sup></b>	Ch. A. - Acids/oxidants	H <sub>3</sub> PO <sub>4</sub> / Pine sawdust	Pre-pyrolysis	+	Zhao et al., (2017)
	Ch. A. - Acids/oxidants	H <sub>2</sub> O <sub>2</sub> / Peanut hull hydrochar	Post-hydrothermal treatment	+	Xue et al., (2012)
	Comp. - Metals	Mn / Pine wood	Pre-pyrolysis	+	Wang et al., (2015a)
	Comp. - Metals	Mn / Pine wood	Post-pyrolysis	+	Wang et al., (2015a)
	Comp. - Metals	Fe / Several feedstocks	Post-pyrolysis	+	Mohan et al.,(2014); Trakal et al., (2016)

	Comp. - Metals	Mg / Cypress sawdust	Pre-pyrolysis	+	Jellali et al., (2016)
	Comp. - C materials	Carbon nanotubes / Sugarcane bagasse	Pre-pyrolysis	=	Inyang et al., (2015)
	Comp. - C materials	Carbon nanotubes / Hickory chips	Pre-pyrolysis	+	Inayng et al., (2015)
	Comp. - Organics	Chitosan / Bamboo, hickory wood	Post-pyrolysis	+	Zhou et al., (2013)
	Comp. - Organics	Chitosan / Sugarcane bagasse, peanut hull	Post-pyrolysis	-	Zhou et al., (2013)
	Comp. - Organics	Chitosan + ZVI particles / Bamboo	Post-pyrolysis	+	Zhou et al., (2014)
<b>NH<sub>4</sub><sup>+</sup></b>	Ch. A. - Acids/oxidants	HNO <sub>3</sub> + NaOH / Corncob waste	Post-pyrolysis	+	Vu et al., (2017)
	Comp. - Clays	Montmorillonite / Bamboo	Pre-pyrolysis	+	Chen et al., (2017)
	Comp. - Clays	Bentonite / Cassava peel	Pre-pyrolysis	+	Ismadji et al., (2016)
<b>NO<sub>3</sub><sup>-</sup></b>	Comp. - Metals	Mg / Several feedstocks	Pre-pyrolysis	+	Zhang et al., (2012)
<b>PO<sub>4</sub><sup>3-</sup></b>	Comp. - Metals	Fe / Several feedstocks	Post-pyrolysis	+	Ren et al., (2015); Micháleková-Richveisová et. al (2017)
	Comp. - Metals	Fe / Several feedstocks	Pre-pyrolysis	+	Cai et al.,(2017); Chen et al., (2011)
	Comp. - Metals	Mg / Several feedstocks	Pre-pyrolysis	+	Yu et al.,(2016); Zhang et al., (2012)
	Comp. - Metals	Mg-enriched tomato	Pre-pyrolysis	+	Yao et al., (2013)
	Comp. - Metals	Ca / Ramie biomass	Pre-pyrolysis	+	Liu et al., (2016)
	Comp. - Electromodified	Al electrode / <i>Laminaria japonica</i>	Pre-pyrolysis	+	Jung et al.,(2015a; 2015b; 2016a)
	Comp. - Clays	Montmorillonite / Bamboo	Pre-pyrolysis	+	Chen et al., (2017)
	Comp. - Clays	Layered double hydroxides / Cotton wood	Post-pyrolysis	+	Zhang et al., (2013b)
	Comp. - Organics	Chitosan + ZVI particles / Bamboo	Post-pyrolysis	+	Zhou et al., (2014)
	Comp. - Microorganisms	Indigenous microbial community / Several feedstocks	Post-pyrolysis	+	Frankel et al., (2016)
<b>As (V)</b>	Ch. A. - Bases	KOH / Municipal solid wastes	Post-pyrolysis	+	Jin et al., (2014)
	Comp. - Metals	Fe / Several feedstocks	Pre-pyrolysis	+	Hu et al,(2015); Zhang et

	Comp. - Metals	Fe / Several feedstocks	Post-pyrolysis	+	al.,(2016); Zhang et al., (2013a) Agrafioti et al.,(2014); Fristak et al.,(2017); Wang et al.,(2015b); Wang et al., (2017b)
	Comp. - Metals	Magnetic gelatin / Chestnut shell	Post-pyrolysis	+	Zhou et al., (2017b)
	Comp. - Metals	Al / Several feedstocks	Pre-pyrolysis	+	Zhang and Gao, (2013)
	Comp. - Metals	Mn / Pine wood	Pre-pyrolysis	+	Wang et al.,(2015a);
	Comp. - Metals	Mn / Pine wood	Post-pyrolysis	+	Wang et al.,(2015a);
	Comp. - Metals	Mn + Ni / Pine wood	Pre- and post-pyrolysis	+	Wang et al., (2016)
	Comp. - Organics	Chitosan + ZVI particles / Bamboo	Post-pyrolysis	+	Zhou et al., (2014)
	Comp. - Microorganisms	Indigenous microbial community / Several feedstocks	Post-pyrolysis	+	Frankel et al., (2016)
	Comp. - Metals	Fe / Rice straw	Post-pyrolysis	+	Quian et al.,(2017); Wang et al., (2017a)
	Comp. - Metals	Fe / Eucalyptus	Post-pyrolysis	-	Wang et al., (2014)
<b>Cr (VI)</b>	Comp. - C materials	Graphene oxide / Hyancith	Pre-pyrolisis	+	Shang et al., (2016)
	Comp. - Organics	Ployethylenimine-methanol / Rice husk	Post-pyrolysis	+	Ma et al., (2014)
	Comp. - Organics	Chitosan / Fe-treated <i>Eichhornia crassipes</i>	Post-pyrolysis	+	Zhang et al., (2015)
	Comp. - Organics	Chitosan + ZVI particles / Bamboo	Post-pyrolysis	+	Zhou et al., (2014)

257

258        **5.1. Activation**

259        The activation of biochar involves the use of steam or acidic or alkaline solutions to create a  
260        network of interconnecting micropores that ultimately increases the surface area upon which  
261        metal cations can chemically or physically adsorb. Physical activation methods force high  
262        temperature steam through the pores of the biochar, which increases the surface area, while  
263        chemical activation methods expose the biochar to acidic or alkaline solutions which oxidise  
264        the surface and create oxygen-containing functional groups (Figure 3).

265        **5.1.1. Physical activation**

266        **5.1.1.1. Steam**

267        Steam activation is a common modification method used to increase the structural porosity of  
268        the biochar and remove impurities such as products of incomplete combustion. This treatment  
269        serves to increase the surface area upon which sorption can occur. Lima and Marchall (2005)  
270        produced activated biochars from poultry manure feedstocks by pyrolysing at 700 °C  
271        followed by steam activation at 800 °C with a range of water flow rates and durations. Higher  
272        flow rates and longer activation times increased the sorption of Cd, Cu and Zn on the surface  
273        of the biochar.

274        Although steam activation increases the surface area and porosity of biochar, Shim et al.  
275        (2015) found that the Cu<sup>2+</sup> sorption capacity of biochar produced by slow pyrolysis of  
276        *Miscanthus* at 500 °C was not significantly changed by activation with steam at 800°C. They  
277        found that although steam activation of the biochar increased the surface area, the abundance  
278        of functional groups decreased, alongside an increase in aromaticity. Similarly, Lou et al.  
279        (2016) observed that steam activation of biochar prepared with pine sawdust increased the  
280        surface area but had little effect on the characteristics of surface functional groups. The steam  
281        treatment did not affect adsorption capacity for phosphate due to electrostatic repulsion by the  
282        negatively charged surface of biochar. Therefore, in the context of inorganic pollutant



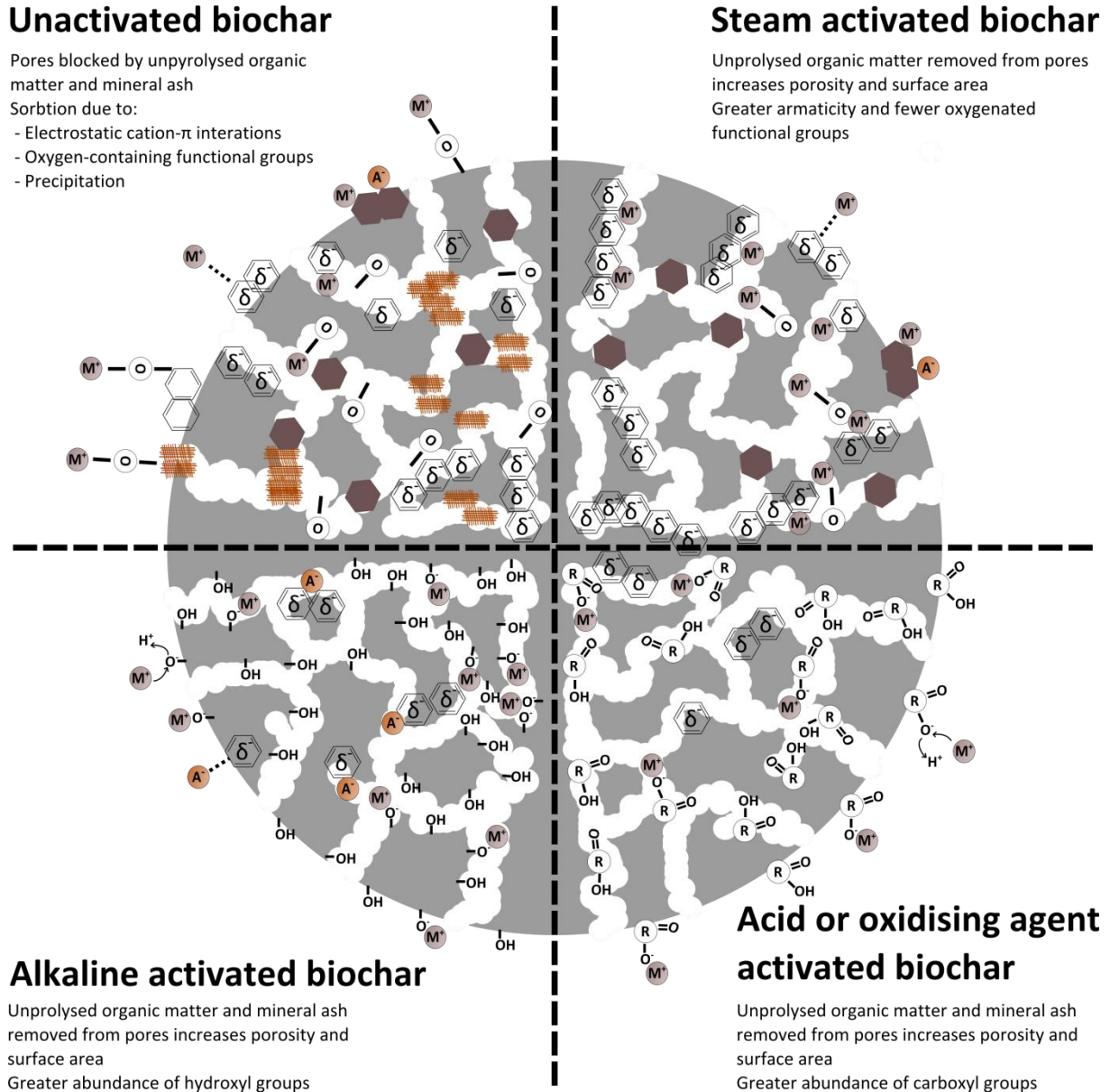
283 sorption, steam activation seems to be more effective when applied prior to a second  
 284 activation/modification step that creates functional groups, as the steam only increases the  
 285 surface area of biochar.

### Unactivated biochar

Pores blocked by unpyrolysed organic matter and mineral ash  
 Sorbtion due to:  
 - Electrostatic cation- $\pi$  interactions  
 - Oxygen-containing functional groups  
 - Precipitation

### Steam activated biochar

Unpyrolysed organic matter removed from pores increases porosity and surface area  
 Greater aromaticity and fewer oxygenated functional groups

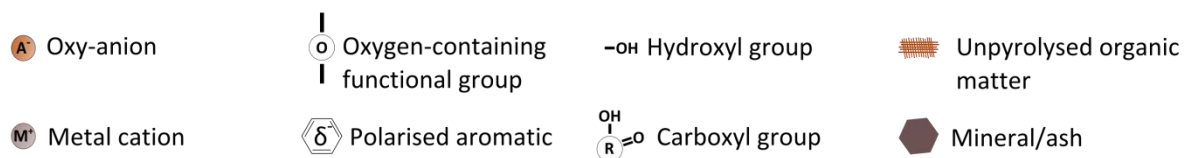


### Alkaline activated biochar

Unpyrolysed organic matter and mineral ash removed from pores increases porosity and surface area  
 Greater abundance of hydroxyl groups

### Acid or oxidising agent activated biochar

Unpyrolysed organic matter and mineral ash removed from pores increases porosity and surface area  
 Greater abundance of carboxyl groups



286  
 287 **Figure 3. Conceptual model identifying the mechanisms of metal cation (e.g. Cd<sup>2+</sup>,**  
 288 **Cu<sup>2+</sup>, Hg<sup>2+</sup>, Pb<sup>2+</sup>, Zn<sup>2+</sup>) and oxyanion (e.g. PO<sub>4</sub><sup>3-</sup>, AsO<sub>4</sub><sup>3-</sup>) sorption to unactivated biochar**  
 289 **and biochar physically activated with steam or chemically activated with acids,**  
 290 **oxidising agents, or alkaline solutions**

## 291        **5.1.2. Chemical activation**

### 292        5.1.2.1. Acids and oxidising agents

293 Biochar surfaces contain several functional groups (e.g. carboxyl, hydroxyl, phenol) that can  
294 chemically bond with metal cations and remove them from solution. Acid treatments provide  
295 more oxygenated functional groups on biochar surfaces and increase the potential for biochar  
296 to chemically bind positively charged pollutants through specific adsorption. The  
297 modification of biochar by exposing the surface to acidic solutions forms carboxylic groups  
298 on the biochar surface (Hadjittofi et al., 2014; Qian et al., 2013) and develops micropores that  
299 lead to an increase in the surface area (Iriarte-Velasco et al., 2016).

300 Hadjittofi et al. (2014) activated a biochar derived from cactus fibres with HNO<sub>3</sub> to increase  
301 the abundance of carboxylic groups on the surface since these groups act as strong Cu<sup>2+</sup>  
302 binding sites. Adsorption was shown to be pH dependent since the sorption capacity of the  
303 resulting biochar was an order of magnitude greater at pH 6.5, compared to pH 3, indicating  
304 chemical sorption on oxygen-containing functional groups on the biochar surface. Oxygen-  
305 containing functional groups were also shown to be incorporated into structure of a rice straw  
306 biochar upon post-pyrolysis treatment with a mixture of H<sub>2</sub>SO<sub>4</sub> and HNO<sub>3</sub>, evidenced by  
307 higher O/C ratios in the final product (Qian et al., 2013).

308 Acid-treatment increased the surface area, the total pore volume and volume of micropores  
309 after treatment of pine tree sawdust with diluted H<sub>3</sub>PO<sub>4</sub> prior to pyrolysis (Zhao et al., 2017).  
310 The incorporation of P-O-P bonds into the C structure increased the Pb sorption capacity of  
311 the phosphoric acid-treated biochar by >20% compared to a non-treated sample due to  
312 phosphate precipitation and surface adsorption (Zhao et al., 2017).

313 Activation of biochar with strong acids can be expensive at large scale and present  
314 environmental issues during the disposal of the activation media, so activation with H<sub>2</sub>O<sub>2</sub>, a  
315 less-expensive and cleaner product has been proposed as an alternative biochar activation

316 medium to increase sorption capacity. Huff et al. (2016) reported an increase in oxygen-  
317 containing functional groups in a pinewood biochar treated with H<sub>2</sub>O<sub>2</sub>. The cation exchange  
318 capacity of the biochar treated with 30% H<sub>2</sub>O<sub>2</sub> almost doubled that of an untreated biochar  
319 since the oxygen-containing functional groups in the surface of biochar, which were more  
320 abundant in the activated biochars, exchanged with cations in solution. Xue et al. (2012)  
321 found that treating a hydrochar with a 10% H<sub>2</sub>O<sub>2</sub> solution increased Pb sorption capacity  
322 compared to the unmodified hydrochar and attributed the increase to a greater abundance of  
323 carboxyl functional groups that can form complexes with Pb. Although Xue et al. (2012)  
324 observed similar mineral compositions in activated and unactivated biochars, the introduction  
325 of acid or oxidising agents dissolves mineral components from within the biochar structure  
326 and removes them from the biochar matrix. These minerals (e.g. P, Ca, Mg, K, Na,) are  
327 particularly important for the removal of metal cations from water by some biochars due to  
328 precipitation (Xu et al., 2013), so some acid treatments may reduce sorption by precipitation.

#### 329 5.1.2.2. Alkaline solutions

330 The most common alkali treatment of biochar is with Group I metal hydroxides (KOH or  
331 NaOH). Activation of biochars with metal hydroxides increases adsorption by increasing  
332 porosity and surface area and by creating of a greater number of oxygenated functional groups  
333 on the surface of the biochar. These oxygenated functional groups provide proton donating  
334 exchange sites upon which metal cations such as Pb<sup>2+</sup> chemically adsorb (Petrović et al.,  
335 2016). Goswami et al. (2016) demonstrated that activation of biochar with KOH, followed by  
336 pyrolysing to 350-550 °C opened up the partially blocked pores and enlarged the diameters of  
337 smaller ones. The KOH and pyrolysis increased the surface area and increased adsorption of  
338 Cd from aqueous solution by surface complexation. Hamid et al. (2014) provided further  
339 evidence that Cu sorption on KOH activated biochar was due to chemical adsorption, as the  
340 kinetics of sorption fitted a pseudo second order model and thermodynamic studies indicated

341 a spontaneous endothermic process. The increase in surface area resulting from modification  
342 of biochar with KOH also increases the adsorption of oxyanions from solution. Jin et al.  
343 (2014) also reported that maximum adsorption capacity of As(V) by biochar produced from  
344 municipal solid wastes was increased 1.3 times from 24 mg/g to 31 mg/g after activation with  
345 2M KOH, due to an increase in surface area and the abundance of functional groups on the  
346 biochar surface. Pietrzak et al. (2014) compared two activation methods using NaOH, which  
347 comprised either pre- or post-pyrolysis activation of feedstock or biochar by physical mixing  
348 or by impregnation with a NaOH solution. The authors reported greater surface area and a  
349 higher iodine sorption capacity when activation was conducted by physical mixing of both the  
350 feedstock and the biochar with solid NaOH.

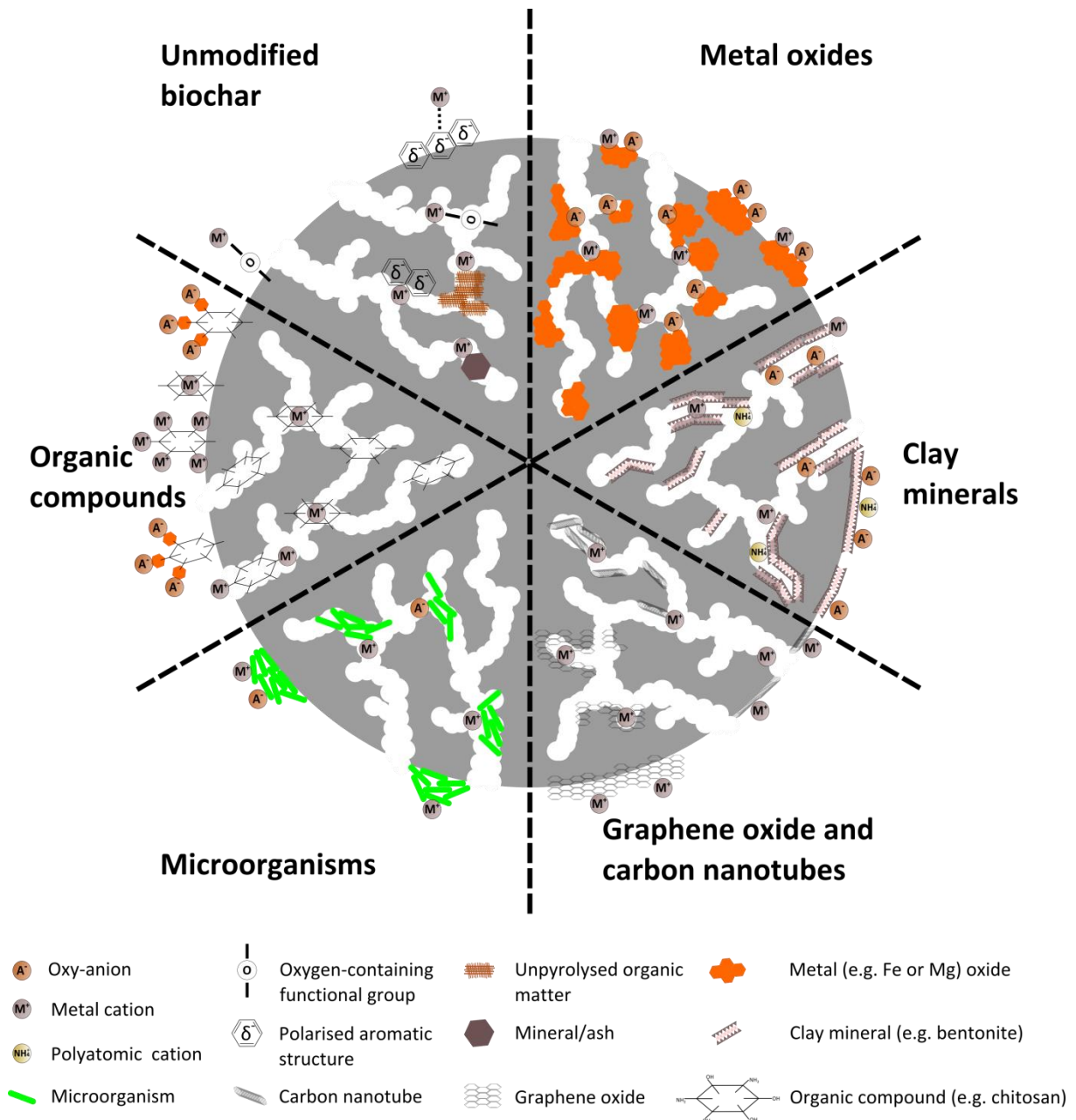
## 351 **5.2. Biochar-based composites**

352 Biochar based composites are produced by impregnating biochar with metal oxides, clays,  
353 organic compounds or carbonaceous materials, such as graphene oxide or carbon nanotubes,  
354 or by inoculation with microorganisms, to alter the surface properties of the biochar (Figure  
355 4). Here the biochar is essentially used as a high-surface-area scaffold to support the materials  
356 being deposited. Composites are distinguished from chemical activation because they involve  
357 the creation of completely new functional groups on surfaces that did not previously exist on  
358 the biochar or feedstock surface.

### 359 **5.2.1. Metal oxides**

360 Biochars generally have a high surface area but a negative surface charge and high pH. These  
361 properties make biochars excellent sorbents for metal cations due to specific adsorption on  
362 oxygenated functional groups, electrostatic attraction to aromatic groups and precipitation on  
363 the mineral ash components of the biochar (Beesley et al., 2015), but poor sorbents for  
364 oxyanion contaminants (e.g.  $\text{NO}_3^-$ ,  $\text{PO}_4^{3-}$  and  $\text{AsO}_4^{3-}$ ). By exploiting the high surface area of  
365 biochars as a platform to embed a metal oxide with contrasting chemical properties (and

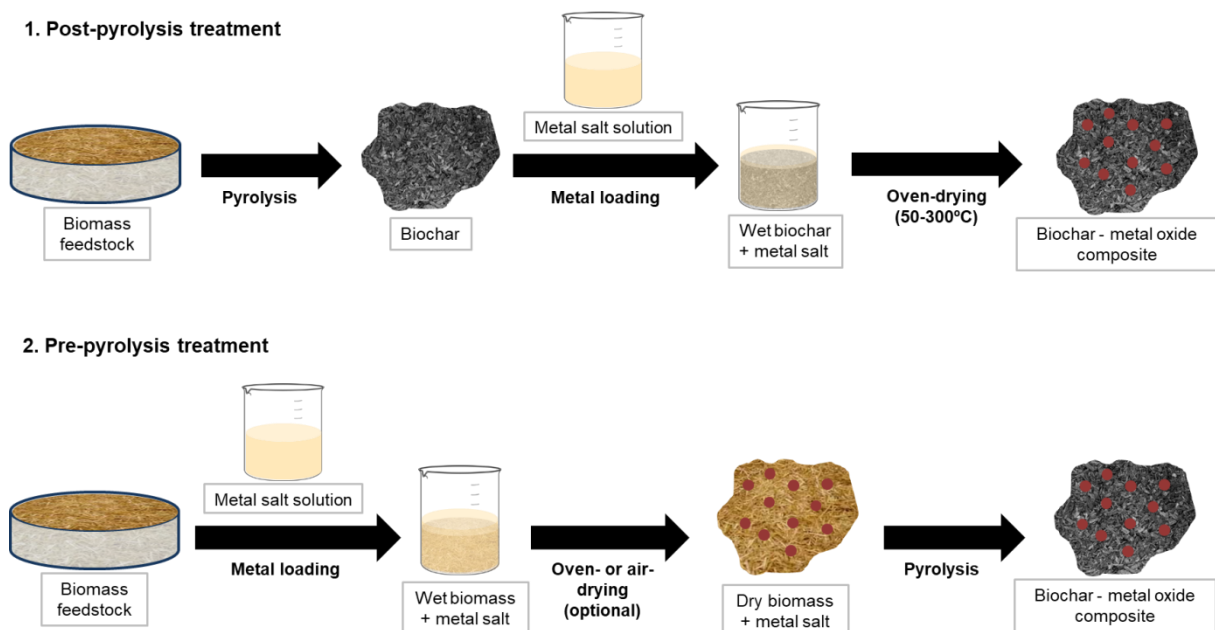
366 usually a positive charge), biochar-based composites are capable of removing negatively  
 367 charged oxyanions from aqueous solutions. The objective of most methodologies to create  
 368 metal oxide biochar-based composites is to ensure a homogenous spread of the metal over the  
 369 biochar surface. The biochar is essentially used as a porous carbon scaffold upon which metal  
 370 oxides precipitated to increase the surface area of the metal oxide.



371  
 372 **Figure 4. Conceptual model identifying the mechanisms of metal cation (e.g. Cd<sup>2+</sup>,**  
 373 **Cu<sup>2+</sup>, Hg<sup>2+</sup>, Pb<sup>2+</sup>, Zn<sup>2+</sup>), oxyanion (e.g. PO<sub>4</sub><sup>3-</sup>, AsO<sub>4</sub><sup>3-</sup>) and polyatomic cation (e.g. NH<sub>4</sub><sup>+</sup>)**  
 374 **sorption to unmodified biochar and biochar modified with metal oxides, clay minerals,**  
 375 **carbonaceous materials (graphene oxide and carbon nanotubes), microorganisms,**  
 376 **and organic compounds.**

377 Generally, impregnation of biochar with metal oxides is performed by soaking biochars or  
 378 their feedstocks in solutions of metal nitrate or chloride salt solutions (Figure 5). The most  
 379 frequently used impregnation agents in the literature are  $\text{FeCl}_3$ ,  $\text{Fe}^0$ ,  $\text{Fe}(\text{NO}_3)_3$  and  $\text{MgCl}_2$ .  
 380 After soaking biochar with metal salt solutions, the biochar is heated under atmospheric  
 381 conditions (i.e. not low-oxygen conditions) at temperatures 50-300 °C to allow nitrates or  
 382 chlorides to be driven off as  $\text{NO}_2$  and  $\text{Cl}_2$  gases and convert the metal ions to metal oxides.

383 Agrafioti et al. (2014) demonstrated that soaking rice husk and municipal waste biomass  
 384 biochars in  $\text{CaO}$ , iron powder and  $\text{FeCl}_3$  prior to pyrolysis created  $\text{Ca}$ ,  $\text{Fe}^0$  and  $\text{Fe}^{3+}$  modified  
 385 biochars, respectively. These modifications increased the capability of the biochars to remove  
 386  $\text{As}(\text{V})$ , but not  $\text{Cr}(\text{VI})$ , from aqueous solution. This observation is supported by Fristak et al.  
 387 (2017) who revealed a 20-fold increase in the sorption of As when corncob biochar was  
 388 modified with  $\text{Fe}(\text{NO}_3)_3$  after pyrolysis, but that the modification had negligible effect on  
 389 sorption of the cationic lanthanide Eu.



390  
 391 **Figure 5. Diagram outlining the pre-pyrolysis and post-pyrolysis procedures used to**  
 392 **modify biochars with metal salts to create metal oxide biochar-based composites.**

393

394 Most metal oxide modifications result in a reduction in the surface area of the biochar due to  
395 clogging of pores with metal oxide precipitates (Rajapaksha et al., 2016; Zhou et al., 2017a).  
396 Micháleková-Richveisová et al. (2017) used the same method as Fristak et al. (2017) to  
397 modify biochars made from garden wood waste and wood chips as well as corncob, which  
398 resulted in a decrease in the surface area of the biochar due to the filling of micro- and  
399 mesopores with Fe. However, despite the lower surface area, modification increased  $\text{PO}_4^{3-}$   
400 sorption capacity by a factor of 12 to 50 due to pH-dependent binding to positively charged  
401 functional groups on the biochar surface.

402 Several attempts have been made to exploit the magnetic properties of Fe to create magnetic  
403 biochars that are capable of removing both metal cation (Mohan et al., 2014) and oxyanion  
404 pollutants (Zhou et al., 2014) from contaminated media. The magnetic property of modified  
405 biochars enables the pollutant-loaded biochar to be removed from the media using a magnet.  
406 Wang et al. (2015b) created a magnetic biochar by pyrolysing pinewood biomass with  
407 hematite, a natural iron-oxide mineral, resulting in an As sorption capacity almost double that  
408 of the unmodified biochar. The modification of biochar to improve magnetic properties was  
409 developed further by Zhou et al. (2017b) by coating with a magnetised gelatin. The authors  
410 observed a 2.6 times increase in the maximum adsorption of As(V) from solution after  
411 biochar modification, attributed to the high electrostatic affinity of As(V) to iron-oxide  
412 particles and protonated oxygen-containing functional groups present on the biochar surface.

413 Biochar-based composites have also been produced by embedding oxides of Al, Mn and Mg  
414 on biochars and improving the sorption of both oxyanions (primarily As and P) and metal  
415 cations (particularly Pb). Zhang and Gao (2013) produced a biochar with high adsorption  
416 capacity for As and P from solution by modification with  $\text{AlCl}_3$  to create a biochar- $\text{AlOOH}$   
417 nanocomposite, Wang et al. (2015a) modified biochar using  $\text{MnCl}_2$  and found that, compared  
418 to the control, the manganese oxide-modified biochar displayed significantly improved

419 sorption capacity for As and Pb. Zhang et al. (2012) compared the modification of biochar  
420 produced from 5 different feedstocks by soaking the biochar in MgCl<sub>2</sub> and applying further  
421 thermal treatment at 600°C. The MgO content in the modified biochars ranged from 8.3% to  
422 26.1%, and the increased adsorption capacity for PO<sub>4</sub><sup>3-</sup> and NO<sub>3</sub><sup>-</sup> was attributed to the positive  
423 charge of the MgO that precipitated on the biochar surfaces. The potential of Mg-modification  
424 to increase the adsorption potential of biochar for metal cations was further explored by Jellali  
425 et al. (2016), who compared the adsorption of lead from solution by a biochar treated with  
426 MgCl<sub>2</sub> prior to pyrolysis to that of unpyrolysed cypress sawdust. The maximum adsorption  
427 capacity of the Mg-modified biochar was approximately 7.4 times higher than that of the  
428 sawdust.

429 Generally the sorption of oxyanions (PO<sub>4</sub><sup>3-</sup> and AsO<sub>4</sub><sup>3-</sup>) on the surface of metal oxide biochar-  
430 based composites is due to chemical adsorption or electrostatic attraction to the positively  
431 charged metal oxide embedded on the surface (Ren et al., 2015; Zhou et al., 2014), whereas  
432 sorption of cationic metals is due to chemical adsorption on oxygenated functional groups on  
433 parts of the biochar that remain unmodified (Tan et al., 2015), or co-precipitation within the  
434 metal oxide lattice (Zhou et al., 2017a).

#### 435 5.2.1.1. Modification of living feedstock biomass

436 Yao et al. (2013) demonstrated an innovative method of biochar modification by irrigating  
437 tomato plants with Mg solution and subsequently pyrolysing the biomass to yield a Mg-rich  
438 biochar with an improved adsorption capacity for PO<sub>4</sub><sup>3-</sup>, compared to the control. The results  
439 showed a strong correlation between the removal rate of P and the concentration of Mg in the  
440 biochar. While interesting, this modification methodology is time consuming, and may be  
441 prohibitively expensive.



#### 442 5.2.1.2. **Electro-modification**

443 The efficiency and homogeneity of metal oxide deposition on the surface of biochar can be  
444 improved by using an electric field to evenly deposit metal ions from the electrodes and the  
445 electrolyte on the surface of the biochar. The application of an electrical field, using an Al  
446 electrode to a solution containing a NaCl electrolyte deposited nano-sized aluminium crystals  
447 of beochemite (AlOOH) on the surface of a marine macroalgae feedstock prior to pyrolysis  
448 (Jung et al., 2015a). The resulting electro-modified biochar had a 45 times greater surface  
449 area, and a well developed microporous structure, most likely due to the generation of strong  
450 oxidising agents (HOCl and OCl<sup>-</sup>) from the NaCl electrolyte. Maximum PO<sub>4</sub><sup>3-</sup> sorption  
451 capacity trebled, compared to the unmodified biochar. The optimum preparation parameters  
452 were later identified for this electro-modification method as a current density of 39 mA/cm<sup>2</sup>, a  
453 pyrolysis temperature of 584 C°, at a heating rate of 6.91 °C/min (Jung et al., 2016a). Electro-  
454 modification was further exploited by Jung et al. (2015b) to prepare Mg/Al-biochar based  
455 nanocomposites by using an Al electrode and MgCl<sub>2</sub> as an electrolyte, which increased the  
456 PO<sub>4</sub><sup>3-</sup> sorption capacity by a factor of ~28, compared to the previous paper. The use of electro-  
457 modification not only results in a more homogenous distribution of metal oxides over the  
458 surface of the biochar, but also considerably decreases the time required to create metal oxide  
459 biochar based composites from a few hours to a few minutes.

#### 460 5.2.2. **Clay minerals**

461 Impregnation of biochars with clay minerals, such as kaolinite, montmorillonite or bentonite,  
462 can modify biochar composition and physical properties, resulting in enhanced sorption  
463 capacity for oxyanions (e.g. PO<sub>4</sub><sup>3-</sup>) and polyatomic cations (e.g. NH<sub>4</sub><sup>+</sup>). To prepare clay  
464 mineral biochar-based composites, the feedstock is generally mixed with a suspension of the  
465 clay mineral prior to pyrolysis (Chen et al., 2017; Ismadji et al., 2016; Rawal et al., 2016; Yao  
466 et al., 2014). Pre-pyrolysis mixing of bamboo with clay minerals (bentonite and kaolinite)

467 mixed with iron sulphate resulted in the incorporation of mineral phases into the biochar  
468 structure, revealed by high contents of Al, Fe and S in the modified biochar (Rawal et al.,  
469 2016). Similarly, Yao et al. (2014) reported increased contents of Al, Fe and Na in  
470 montmorillonite and kaolinite biochar composites produced from plant biomass feedstocks  
471 (bamboo, bagasse and hickory chips), indicating successful incorporation of both clay  
472 minerals into the biochar structure. X-ray diffraction analysis of a bentonite biochar-based  
473 composite produced by pyrolysis of cassava peel and bentonite revealed the typical basal  
474 spacing of the crystalline structure of the bentonite along with the amorphous structure of the  
475 biochar, indicating that bentonite structure remained after pyrolysis (Ismadji et al., 2016).

476 Chen et al. (2017) observed that mixing bamboo powder with montmorillonite prior to  
477 pyrolysis increased the surface area and the pore volume and diameter, partly due to the  
478 presence of layered montmorillonite. Layered surfaces have been observed by Scanning  
479 Electron Microscope imaging of clay modified biochar, resembling common clay structure  
480 morphology (Yao et al., 2014). However, high pyrolysis temperatures can lead to loss of  
481 structural water from the clay mineral, reducing the interlayer space of montmorillonite and  
482 ultimately reducing the pore diameter and volume of the modified biochar (Chen et al., 2017;  
483 Ismadji et al., 2016; Rawal et al., 2016).

484 The increased surface area of a montmorillonite modified biochar resulted in a greater  
485 adsorption capacity for  $\text{NH}_4^+$  and  $\text{PO}_4^{3-}$ , compared to an unmodified biochar, but showed a  
486 stronger affinity for  $\text{PO}_4^{3-}$  than for  $\text{NH}_4^+$  (Chen et al., 2017).  $\text{NH}_4^+$  was mainly controlled by  
487 Van der Waals forces and partially by cation exchange, whereas phosphate was adsorbed  
488 through electrostatic interaction and ionic bonding between  $\text{PO}_4^{3-}$  and cations present in the  
489 montmorillonite (Chen et al., 2017). The maximum adsorption capacity was 12.5 mg/g for  
490  $\text{NH}_4^+$  and 105 mg/g for  $\text{PO}_4^{3-}$  and slow-release behaviours were exhibited for both these

491 nutrients, indicating a potential market for the saturated biochar-composite as a slow-release  
492 fertiliser.

493 A bentonite-biochar composite produced from cassava peel and activated with CO<sub>2</sub> at the  
494 final pyrolysis stage, presented ~150% greater sorption capacity for NH<sub>4</sub><sup>+</sup> than an unmodified  
495 biochar (Ismadji et al., 2016). This increase is ascribed to enhanced physical adsorption of  
496 NH<sub>4</sub><sup>+</sup> onto the surface of bentonite-biochar composite, together with its exchange with cations  
497 present in the interlayer of bentonite and a more developed microporosity due to activation  
498 with CO<sub>2</sub>.

499 Deposition of MgAl-layered double hydroxides (LDH), as anionic clay minerals, within the  
500 biochar matrix increased the PO<sub>4</sub><sup>3-</sup> sorption capacity of the resulting biochar-based composite  
501 with respect to unmodified biochars and other LDHs used as adsorbents. The enhanced  
502 phosphate adsorption was due to successful deposition and separation of the LDH nanosized  
503 particles on the biochar surface and increased sorption capacity either through anion exchange  
504 or surface adsorption (Zhang et al., 2013b).

### 505 **5.2.3. Coating with carbonaceous materials (graphene oxide and carbon nanotubes)**

506 Graphene oxide is a widely used precursor for the production of graphene and has shown  
507 great sorption capacity for metals, such as Cd<sup>2+</sup>, Co<sup>2+</sup>, Cu<sup>2+</sup>, Pb<sup>2+</sup> and Zn<sup>2+</sup>, which chemically  
508 bind with the oxygen-containing groups present on the graphene oxide surface (Ren et al.,  
509 2012; Sitko et al., 2013; Zhao et al., 2011). Graphene oxide-biochar composites have been  
510 used to improve biochar sorption capacity (Shang et al., 2016; Tang et al., 2015). These  
511 composites are prepared by impregnation of the feedstock in a graphene oxide suspension  
512 before pyrolysis, which generally increases the surface area and creates more oxygen-  
513 containing functional groups than the unmodified biochar due to the incorporation of the  
514 graphene structure in the composite after pyrolysis (Shang et al., 2016; Tang et al., 2015).

515 Shang et al. (2016) found that Cr(VI) removal efficiency from aqueous solution by graphene  
516 oxide biochar-based composite prepared from hyacinth biomass was considerably higher than  
517 that of an unmodified biochar. The authors suggested that Cr(VI) sorption onto the composite  
518 was likely via electrostatic attraction of Cr(VI) coupled with Cr(VI) reduction to Cr(III) and  
519 Cr(III) complexation (Shang et al., 2016). Tang et al. (2015) mixed wheat straw with a  
520 suspension of graphene oxide at different biomass:graphene oxide ratios (0.1%, 0.5% and  
521 1%) prior to slow pyrolysis at 600 °C and studied the graphene oxide-biochar composite  
522 sorption characteristics for Hg<sup>2+</sup> in aqueous solution. The Hg<sup>2+</sup> removal efficiency increased  
523 with increasing the proportions of graphene oxide in the composite, with the highest load of  
524 graphene oxide (1%) removing 8.7% more Hg<sup>2+</sup> from solution than the unmodified biochar.  
525 Fourier transform infrared spectroscopy indicated that mercury was primarily bound by  
526 oxygen-containing functional groups on the graphene oxide-biochar composite.

527 Biochar coated with carbon nanotubes (CNT) has been also synthesized and evaluated for its  
528 metal cation sorption capacity (Inyang et al., 2014; Inyang et al., 2015). For the CNT-biochar  
529 composites preparation, the biomass feedstock (sugarcane bagasse or hickory chips) was  
530 mixed with a CNT suspension, stirred, and oven-dried prior to pyrolysis. CNT were  
531 successfully incorporated to the biochar structure, resulting in higher surface area and pore  
532 volume and increasingly negatively charged surface with increasing CNT loading (Inyang et  
533 al., 2014). Improvement of Pb<sup>2+</sup> sorption capacity with the CNT coating treatment was only  
534 observed when hickory was used as a feedstock, whereas no effect was found for the  
535 sugarcane biochar (Inyang et al., 2015). However, mixing the CNT with a surfactant (sodium  
536 dodecyl benzene sulfonate) prior to biomass impregnation improved the Pb<sup>2+</sup> removal  
537 efficiency of both CNT-biochar composites (Inyang et al., 2015). Pb<sup>2+</sup> was likely adsorbed  
538 through interaction (chemical binding or electrostatic attraction) with oxygen-containing  
539 groups in CNT-biochar composite surface (Inyang et al., 2015).

540        **5.2.4. Microorganisms**

541 Biochar provides a high surface area inert material to support the colonisation and growth of  
542 biofilms with desirable properties. The inoculation of microorganisms onto the surface of  
543 biochars has primarily been attempted to facilitate the biodegradation of organic  
544 contaminants, which is beyond the scope of this review. However, alongside biodegradation  
545 of naphthenic acids, Frankel et al. (2016) observed biosorption of metals from solution by  
546 biofilms on biochars colonised by microorganisms isolated from oil sands process water.  
547 Sorption of P and As was up to 6 and 7 times greater than uncolonised biochar, respectively,  
548 and up to 4 or 5 times greater than colonised and sterilised biochar.

549        **5.2.5. Organic compounds**

550 Biochars can be modified post-pyrolysis with organic compounds with functional groups that  
551 are capable of creating strong bonds with both the surface of the biochar and also pollutants  
552 from solution. Incorporation of amino groups onto the surface of biochar can enhance the  
553 pollutant sorption capacity by inducing strong complexation with the amino moieties. This  
554 modification can be achieved either by simple chemical reactions (Yang & Jiang, 2014) or by  
555 mixing biochars with polymers rich in amino groups, such as polyethylenimine or chitosan  
556 (Ma et al., 2014; Zhang et al., 2015; Zhou et al., 2014; Zhou et al., 2013).

557 Yang and Jiang (2014) prepared an amino-modified biochar with a commercial saw dust  
558 biochar by nitrification through electrophilic substitution reaction, using HNO<sub>3</sub> and H<sub>2</sub>SO<sub>4</sub>,  
559 followed by reduction with Na<sub>2</sub>S<sub>2</sub>O<sub>4</sub>. Although no significant differences in the physical  
560 structure were found between the modified and unmodified biochar, the surface of the  
561 modified biochar had more functional groups, especially those associated to the amino  
562 moieties. The amino-modification resulted in 5 times greater Cu<sup>2+</sup> sorption capacity which was  
563 strongly complexed by the amino groups present on the modified biochar surface (Yang &  
564 Jiang, 2014).

565 A rice-husk biochar, pre-treated with acid or alkali solutions, modified by mixing with  
566 polyethylenimine (PEI)/methanol solution, had a greater abundance of functional groups on  
567 its surface and was richer in N and O, confirming the incorporation of PEI to the structure  
568 (Ma et al., 2014). The presence of more amine functional groups enhanced the sorption  
569 capacity of the modified biochar for Cr(VI), which was partially reduced to Cr(III) during  
570 adsorption (Ma et al., 2014).

571 Zhou et al. (2013) prepared chitosan-biochar composites by mixing biochars produced from  
572 bamboo, sugarcane bagasse, hickory wood and peanut hull feedstocks with an acid chitosan  
573 solution. The composites had a smaller surface area than the unmodified biochars, probably  
574 due to the pore blockage by the incorporation of chitosan in the biochar structure, which was  
575 confirmed by higher N, H and O contents. Generally, modification with chitosan increased the  
576 metal cation sorption capacity of biochars, although some exceptions were found probably  
577 related to the lower surface area. Pb adsorption isotherms of chitosan modified bamboo  
578 biochar and characterisation Pb-laden composites suggested that Pb was adsorbed primarily  
579 due to an interaction with amine functional groups of chitosan (Zhou et al., 2013).

580 Chitosan has been also applied to improve the impregnation of biochars with metal oxides to  
581 produce magnetic biochars (Zhang et al., 2015; Zhou et al., 2014). When mixed with a  $\gamma$ -  
582 Fe<sub>2</sub>O<sub>3</sub>-biochar composite, more functional groups were incorporated into the chitosan-  $\gamma$ -  
583 Fe<sub>2</sub>O<sub>3</sub>-biochar composite, which showed promising results concerning Cr(VI) sorption from  
584 aqueous solution (Zhang et al., 2015). Similarly, a modified biochar produced using bamboo  
585 biochar, chitosan and zero valent iron (ZVI) particles at various ratios, showed much higher  
586 removal efficiency for Pb<sup>+2</sup>, Cr(VI), As(V) and P than the unmodified biochar (Zhou et al.,  
587 2014). Coating biochar with chitosan alone (with no ZVI addition) enhanced the removal  
588 efficiency of Pb<sup>+2</sup> and Cr(VI) due to the complexation capacity of the amine functional groups  
589 of chitosan, but the presence of ZVI further improved the removal of these metals. Whereas

590 the chitosan-only modified BC showed no sorption capacity for As(V) and P, the presence of  
591 ZVI in the composite greatly increased the removal efficiency of As(V) and P, likely  
592 adsorbed by electrostatic interactions with ZVI particles (Zhou et al., 2014).

## 593 **6. Future work**

594 Further development work will mainly optimise the choice of feedstock, pyrolysis  
595 temperature, and conditions under which biochars are modified (e.g. temperature, rate,  
596 concentration and choice of chemical compound, solid:solution ratio, mixing) in order to  
597 obtain a versatile suite of enhanced biochars with highly predictable properties that can be  
598 applied to multiple remediation scenarios. New developments should seek to find  
599 compromises between the biochar feedstock, modification method and sorption performance  
600 that minimises costs and maximises the breadth of technical applicability, while maintaining  
601 long-term performance.

602 Biochar modification will inevitably raise the production costs, thus the profitability of using  
603 modified biochars compared to other materials, such as activated carbons, as adsorbents  
604 should be analysed for each specific case. The production and application costs of biochar as  
605 adsorbent for pollutants in aqueous solutions depends on multiple factors that present some  
606 uncertainties and can vary considerably. These include the origin and availability of the  
607 feedstock; preparation of the raw material (cleaning, drying); costs of biochar production,  
608 which will depend largely on pyrolysis conditions (slow vs fast, temperature); distribution  
609 costs; the environmental impact and lifetime and regeneration after use (Alhashimi & Aktas,  
610 2017). The economical assessment of using any adsorbent should also consider its efficiency  
611 for a given contaminant or material. Physical activation of biochar would increase the energy  
612 consumption costs, whereas chemical activation and production of biochar-based composites  
613 would also include the price of reagents (Banerjee et al., 2016). In these cases, a particularly  
614 challenging aspect of future optimisation is to decrease the quantity of chemicals required to

615 activate or modify the biochar produced to minimise costs of production while maintaining  
616 maximum sorption capacity by optimising the biochar:modifying agent ratio .

617 There is a considerable opportunity to develop biochars that act as scaffolds for nano-  
618 adsorbents which have received increasing research attention recently (Kyzas & Matis, 2015).  
619 Creating biochar-based nano-adsorbents would offer a huge potential to develop adsorbent  
620 nano-materials with a high surface area and a specific surface functionality while using as  
621 little materials as possible.

622 The stability of biochar-based composite modifications over time should be monitored in  
623 future experiments as some of the materials imbibed in the biochar matrix (e.g. metal  
624 compounds, C nanotubes, organic compounds) can leach away from the biochar if they are  
625 not well fixed. To address this issue, leaching tests are required. One scenario worthy of  
626 investigation is the stability of metal-biochar composites in acidic solutions (pH 4-5), to  
627 determine whether metals are released from the biochar matrix.

628 Another gap is the ecotoxicology of these new biochar formulations. Biochar itself has been  
629 shown to be good for environmental applications, but sometimes has been shown to contain  
630 toxic compounds (Soudek et al., 2016). Modifying or activating the biochar leads to chemical  
631 and physical changes that could potentially increase the toxicity (reactivity, presence of  
632 nanoparticles, metals, etc). For example, Shim et al. (2015) pointed out that activated biochars  
633 can induce toxicity to *Daphnia magna*. To ensure environmental protection, the toxicity of  
634 modified biochars needs to be evaluated to avoid undesirable impacts to aquatic organisms  
635 (Gonçalves et al., 2016).

636 Also important is the sustainability of modified biochars and how they may contribute to the  
637 circular economy. A considerable challenge facing the designers of biochars and activated or  
638 modified biochars is to enable the regeneration and re-use of the sorbent so that the ‘pollutant’



639 can be desorbed from the biochar surface and recovered. The biochar may then be used to  
640 adsorb more pollutants from water. This is particularly important when considering disposal  
641 of biochar after it has been used to remediate water. If the saturated biochar is considered  
642 hazardous waste then disposal may be costly and so a re-usable sorbent offers environmental  
643 and economic advantages. If the inorganic pollutant loaded on the biochar cannot be  
644 efficiently desorbed and recovered then the saturated biochar may still be used as a resource.  
645 For example, P and N saturated modified biochars could be of potential use in agriculture  
646 (cropping) or ecological restoration (revegetation) as a slow release fertiliser when applied to  
647 soils (Ismail & Hameed, 2016; Roy, 2016). Accordingly, biochars containing Cu or Zn may  
648 be useful as micronutrient fertilisers.

## 649 **7. Conclusions**

650 The development of methods to modify biochars to enhance their inorganic pollutant sorption  
651 capacity or to expand the breadth pollutants that they can be removed from aqueous solution  
652 is in its infancy. Physical and chemical activation of biochar can increase the surface area and  
653 increase the abundance of oxygenated functional groups to increase cation adsorption.  
654 Embedding materials on the surface of biochar can alter the properties of the surface by  
655 creating biochar-based composites, enabling the adsorption of different pollutants. Research  
656 into biochar-based composites have primarily been progressed by embedding iron or  
657 manganese oxides to increase oxyanion sorption capacity.

658 The E-supplement contains a table which classifies the inorganic contaminants of primary  
659 concern classified by their chemical behavior and includes citations to peer reviewed articles  
660 that identify their sources in water.

661 **8. Acknowledgements**

662 This research did not receive any specific grant from funding agencies in the public,  
663 commercial, or not-for-profit sectors. However, EMJ and GA are thankful to the Cooperation  
664 Program UAM-Banco Santander, grant no. 2017/ASIA/07.

665  
666 **9. References**

- 667 1. Agrafioti, E., Kalderis, D., Diamadopoulos, E. 2014. Ca and Fe modified biochars as  
668 adsorbents of arsenic and chromium in aqueous solutions. *Journal of Environmental*  
669 *Management*, **146**, 444-450.
- 670 2. Ahmad, M., Lee, S.S., Dou, X., Mohan, D., Sung, J.-K., Yang, J.E., Ok, Y.S. 2012.  
671 Effects of pyrolysis temperature on soybean stover-and peanut shell-derived biochar  
672 properties and TCE adsorption in water. *Bioresource technology*, **118**, 536-544.
- 673 3. Alhashimi, H.A., Aktas, C.B. 2017. Life cycle environmental and economic performance  
674 of biochar compared with activated carbon: A meta-analysis. *Resources, Conservation*  
675 *and Recycling*, **118**, 13-26.
- 676 4. Banerjee, S., Mukherjee, S., LaminKa-ot, A., Joshi, S., Mandal, T., Halder, G. 2016.  
677 Biosorptive uptake of Fe 2+, Cu 2+ and As 5+ by activated biochar derived from  
678 *Colocasia esculenta*: Isotherm, kinetics, thermodynamics, and cost estimation. *Journal of*  
679 *advanced research*, **7**(5), 597-610.
- 680 5. Beesley, L., Moreno-Jimenez, E., Fellet, G., Carrijo, L., Sizmur, T. 2015. Biochar and  
681 heavy metals. in: *Biochar for Environmental Management: Science and Technology*,  
682 (Eds.) J. Lehmann, S. Joseph, Routledge. Abingdon, UK.
- 683 6. Cai, R., Wang, X., Ji, X., Peng, B., Tan, C., Huang, X. 2017. Phosphate reclaim from  
684 simulated and real eutrophic water by magnetic biochar derived from water hyacinth.  
685 *Journal of Environmental Management*, **187**, 212-219.
- 686 7. Cantrell, K.B., Hunt, P.G., Uchimiya, M., Novak, J.M., Ro, K.S. 2012. Impact of  
687 pyrolysis temperature and manure source on physicochemical characteristics of biochar.  
688 *Bioresource technology*, **107**, 419-428.
- 689 8. Cao, X., Ma, L., Gao, B., Harris, W. 2009. Dairy-manure derived biochar effectively  
690 sorbs lead and atrazine. *Environmental science & technology*, **43**(9), 3285-3291.
- 691 9. Chen, B., Chen, Z., Lv, S. 2011. A novel magnetic biochar efficiently sorbs organic  
692 pollutants and phosphate. *Bioresource technology*, **102**(2), 716-723.
- 693 10. Chen, L., Chen, X.L., Zhou, C.H., Yang, H.M., Ji, S.F., Tong, D.S., Zhong, Z.K., Yu,  
694 W.H., Chu, M.Q. 2017. Environmental-friendly Montmorillonite-Biochar Composites:  
695 Facile Production and Tunable Adsorption-Release of Ammonium and Phosphate.  
696 *Journal of Cleaner Production*.
- 697 11. Chen, T., Zhang, Y., Wang, H., Lu, W., Zhou, Z., Zhang, Y., Ren, L. 2014. Influence of  
698 pyrolysis temperature on characteristics and heavy metal adsorptive performance of  
699 biochar derived from municipal sewage sludge. *Bioresource technology*, **164**, 47-54.

- 700 **12.** Conley, D.J., Paerl, H.W., Howarth, R.W., Boesch, D.F., Seitzinger, S.P., Havens, K.E.,  
701 Lancelot, C., Likens, G.E. 2009. Controlling eutrophication: nitrogen and phosphorus.  
702 *Science*, **323**(5917), 1014-1015.
- 703 **13.** Ding, W., Dong, X., Ime, I.M., Gao, B., Ma, L.Q. 2014. Pyrolytic temperatures impact  
704 lead sorption mechanisms by bagasse biochars. *Chemosphere*, **105**, 68-74.
- 705 **14.** Dudgeon, D., Arthington, A.H., Gessner, M.O., Kawabata, Z.I., Knowler, D.J., Lévêque,  
706 C., Naiman, R.J., Prieur-Richard, A.H., Soto, D., Stiassny, M.L. 2006. Freshwater  
707 biodiversity: importance, threats, status and conservation challenges. *Biological reviews*,  
708 **81**(2), 163-182.
- 709 **15.** Fletcher, A.J., Smith, M.A., Heinemeyer, A., Lord, R., Ennis, C.J., Hodgson, E.M.,  
710 Farrar, K. 2014. Production factors controlling the physical characteristics of biochar  
711 derived from phytoremediation willow for agricultural applications. *BioEnergy Research*,  
712 **7**(1), 371-380.
- 713 **16.** Frankel, M.L., Bhuiyan, T.I., Veksha, A., Demeter, M.A., Layzell, D.B., Helleur, R.J.,  
714 Hill, J.M., Turner, R.J. 2016. Removal and biodegradation of naphthenic acids by  
715 biochar and attached environmental biofilms in the presence of co-contaminating metals.  
716 *Bioresource technology*, **216**, 352-361.
- 717 **17.** Frišták, V., Micháleková-Richveisová, B., Víglašová, E., Ďuriška, L., Galamboš, M.,  
718 Moreno-Jiménez, E., Pipiška, M., Soja, G. 2017. Sorption separation of Eu and As from  
719 single-component systems by Fe-modified biochar: kinetic and equilibrium study.  
720 *Journal of the Iranian Chemical Society*, **14**(3), 521-530.
- 721 **18.** Gomez-Eyles, J.L., Beesley, L., Moreno-Jimenez, E., Ghosh, U., Sizmur, T. 2013. The  
722 potential of biochar amendments to remediate contaminated soils. *Biochar and Soil*  
723 *Biota*, **4**, 100-133.
- 724 **19.** Gonçalves, S.P.C., Strauss, M., Delite, F.S., Clemente, Z., Castro, V.L., Martinez, D.S.T.  
725 2016. Activated carbon from pyrolysed sugarcane bagasse: Silver nanoparticle  
726 modification and ecotoxicity assessment. *Science of The Total Environment*, **565**, 833-  
727 840.
- 728 **20.** Goswami, R., Shim, J., Deka, S., Kumari, D., Kataki, R., Kumar, M. 2016.  
729 Characterization of cadmium removal from aqueous solution by biochar produced from  
730 *Ipomoea fistulosa* at different pyrolytic temperatures. *Ecological Engineering*, **97**, 444-  
731 451.
- 732 **21.** Hadjittofi, L., Prodromou, M., Pashalidis, I. 2014. Activated biochar derived from cactus  
733 fibres – Preparation, characterization and application on Cu(II) removal from aqueous  
734 solutions. *Bioresource technology*, **159**, 460-464.
- 735 **22.** Hamid, S.B.A., Chowdhury, Z.Z., Zain, S.M. 2014. Base catalytic approach: A  
736 promising technique for the activation of biochar for equilibrium sorption studies of  
737 copper, Cu (II) ions in single solute system. *Materials*, **7**(4), 2815-2832.
- 738 **23.** Harvey, O.R., Herbert, B.E., Rhue, R.D., Kuo, L.-J. 2011. Metal interactions at the  
739 biochar-water interface: energetics and structure-sorption relationships elucidated by  
740 flow adsorption microcalorimetry. *Environmental science & technology*, **45**(13), 5550-  
741 5556.

- 742 **24.** Hu, X., Ding, Z., Zimmerman, A.R., Wang, S., Gao, B. 2015. Batch and column sorption  
743 of arsenic onto iron-impregnated biochar synthesized through hydrolysis. *water research*,  
744 **68**, 206-216.
- 745 **25.** Huff, M.D., Lee, J.W. 2016. Biochar-surface oxygenation with hydrogen peroxide.  
746 *Journal of Environmental Management*, **165**, 17-21.
- 747 **26.** Inyang, M., Gao, B., Zimmerman, A., Zhang, M., Chen, H. 2014. Synthesis,  
748 characterization, and dye sorption ability of carbon nanotube–biochar nanocomposites.  
749 *Chemical Engineering Journal*, **236**, 39-46.
- 750 **27.** Inyang, M., Gao, B., Zimmerman, A., Zhou, Y., Cao, X. 2015. Sorption and cosorption  
751 of lead and sulfapyridine on carbon nanotube-modified biochars. *Environmental Science  
752 and Pollution Research*, **22**(3), 1868-1876.
- 753 **28.** Iriarte-Velasco, U., Sierra, I., Zudaire, L., Ayastuy, J.L. 2016. Preparation of a porous  
754 biochar from the acid activation of pork bones. *Food and Bioproducts Processing*, **98**,  
755 341-353.
- 756 **29.** Ismadji, S., Tong, D.S., Soetaredjo, F.E., Ayucitra, A., Yu, W.H., Zhou, C.H. 2016.  
757 Bentonite hydrochar composite for removal of ammonium from Koi fish tank. *Applied  
758 Clay Science*, **119**, 146-154.
- 759 **30.** Ismail, Z.Z., Hameed, B.B. 2016. Sustainable Application of Agro-industrial Biomass  
760 Waste for Water Treatment: Recycling of Sunflower Seeds Hulls for Ammonium  
761 Removal. *The Journal of Solid Waste Technology and Management*, **42**(4), 251-259.
- 762 **31.** Jellali, S., Diamantopoulos, E., Haddad, K., Anane, M., Durner, W., Mlayah, A. 2016.  
763 Lead removal from aqueous solutions by raw sawdust and magnesium pretreated biochar:  
764 Experimental investigations and numerical modelling. *Journal of Environmental  
765 Management*, **180**, 439-449.
- 766 **32.** Jin, H., Capareda, S., Chang, Z., Gao, J., Xu, Y., Zhang, J. 2014. Biochar pyrolytically  
767 produced from municipal solid wastes for aqueous As (V) removal: Adsorption property  
768 and its improvement with KOH activation. *Bioresource technology*, **169**, 622-629.
- 769 **33.** Jung, K.-W., Hwang, M.-J., Jeong, T.-U., Ahn, K.-H. 2015a. A novel approach for  
770 preparation of modified-biochar derived from marine macroalgae: Dual purpose electro-  
771 modification for improvement of surface area and metal impregnation. *Bioresource  
772 technology*, **191**, 342-345.
- 773 **34.** Jung, K.-W., Jeong, T.-U., Hwang, M.-J., Kim, K., Ahn, K.-H. 2015b. Phosphate  
774 adsorption ability of biochar/Mg–Al assembled nanocomposites prepared by aluminum-  
775 electrode based electro-assisted modification method with MgCl<sub>2</sub> as electrolyte.  
776 *Bioresource technology*, **198**, 603-610.
- 777 **35.** Jung, K.-W., Jeong, T.-U., Kang, H.-J., Chang, J.-S., Ahn, K.-H. 2016a. Preparation of  
778 modified-biochar from *Laminaria japonica*: Simultaneous optimization of aluminum  
779 electrode-based electro-modification and pyrolysis processes and its application for  
780 phosphate removal. *Bioresource technology*, **214**, 548-557.
- 781 **36.** Jung, K.-W., Kim, K., Jeong, T.-U., Ahn, K.-H. 2016b. Influence of pyrolysis  
782 temperature on characteristics and phosphate adsorption capability of biochar derived  
783 from waste-marine macroalgae (*Undaria pinnatifida* roots). *Bioresource technology*, **200**,  
784 1024-1028.

- 785 **37.** Kim, K.H., Kim, J.-Y., Cho, T.-S., Choi, J.W. 2012. Influence of pyrolysis temperature  
786 on physicochemical properties of biochar obtained from the fast pyrolysis of pitch pine  
787 (*Pinus rigida*). *Bioresource technology*, **118**, 158-162.
- 788 **38.** Kim, W.-K., Shim, T., Kim, Y.-S., Hyun, S., Ryu, C., Park, Y.-K., Jung, J. 2013.  
789 Characterization of cadmium removal from aqueous solution by biochar produced from a  
790 giant *Miscanthus* at different pyrolytic temperatures. *Bioresource technology*, **138**, 266-  
791 270.
- 792 **39.** Kotaś, J., Stasicka, Z. 2000. Chromium occurrence in the environment and methods of its  
793 speciation. *Environmental Pollution*, **107**(3), 263-283.
- 794 **40.** Kyzas, G.Z., Matis, K.A. 2015. Nanoadsorbents for pollutants removal: a review.  
795 *Journal of Molecular Liquids*, **203**, 159-168.
- 796 **41.** Lee, J.W., Kidder, M., Evans, B.R., Paik, S., Buchanan Iii, A., Garten, C.T., Brown, R.C.  
797 2010. Characterization of biochars produced from cornstovers for soil amendment.  
798 *Environmental Science & Technology*, **44**(20), 7970-7974.
- 799 **42.** Liang, B., Lehmann, J., Solomon, D., Kinyangi, J., Grossman, J., O'Neill, B., Skjemstad,  
800 J., Thies, J., Luizao, F., Petersen, J. 2006. Black carbon increases cation exchange  
801 capacity in soils. *Soil Science Society of America Journal*, **70**(5), 1719-1730.
- 802 **43.** Lima, I.M., Marshall, W.E. 2005. Adsorption of selected environmentally important  
803 metals by poultry manure-based granular activated carbons. *Journal of Chemical*  
804 *Technology and Biotechnology*, **80**(9), 1054-1061.
- 805 **44.** Liu, S.-b., Tan, X.-f., Liu, Y.-g., Gu, Y.-l., Zeng, G.-m., Hu, X.-j., Wang, H., Zhou, L.,  
806 Jiang, L.-h., Zhao, B.-b. 2016. Production of biochars from Ca impregnated ramie  
807 biomass (*Boehmeria nivea* (L.) Gaud.) and their phosphate removal potential. *RSC*  
808 *Advances*, **6**(7), 5871-5880.
- 809 **45.** Lou, K., Rajapaksha, A.U., Ok, Y.S., Chang, S.X. 2016. Pyrolysis temperature and steam  
810 activation effects on sorption of phosphate on pine sawdust biochars in aqueous  
811 solutions. *Chemical Speciation & Bioavailability*, **28**(1-4), 42-50.
- 812 **46.** Ma, Y., Liu, W.-J., Zhang, N., Li, Y.-S., Jiang, H., Sheng, G.-P. 2014. Polyethylenimine  
813 modified biochar adsorbent for hexavalent chromium removal from the aqueous solution.  
814 *Bioresource technology*, **169**, 403-408.
- 815 **47.** Micháleková-Richveisová, B., Frišták, V., Pipíška, M., Ďuriška, L., Moreno-Jimenez, E.,  
816 Soja, G. 2017. Iron-impregnated biochars as effective phosphate sorption materials.  
817 *Environmental Science and Pollution Research*, **24**(1), 463-475.
- 818 **48.** Mohan, D., Kumar, H., Sarswat, A., Alexandre-Franco, M., Pittman Jr, C.U. 2014.  
819 Cadmium and lead remediation using magnetic oak wood and oak bark fast pyrolysis  
820 bio-chars. *Chemical Engineering Journal*, **236**, 513-528.
- 821 **49.** Moore, J.W., Ramamoorthy, S. 2012. *Heavy metals in natural waters: applied*  
822 *monitoring and impact assessment*. Springer Science & Business Media.
- 823 **50.** Mueller, D.K., Helsel, D.R. 1996. Nutrients in the nation's waters: too much of a good  
824 thing?
- 825 **51.** Mukherjee, A., Zimmerman, A.R., Harris, W. 2011. Surface chemistry variations among  
826 a series of laboratory-produced biochars. *Geoderma*, **163**(3-4), 247-255.

- 827 **52.** Niu, Q., Luo, J., Xia, Y., Sun, S., Chen, Q. 2017. Surface modification of bio-char by  
828 dielectric barrier discharge plasma for Hg 0 removal. *Fuel Processing Technology*, **156**,  
829 310-316.
- 830 **53.** Paethanom, A., Yoshikawa, K. 2012. Influence of pyrolysis temperature on rice husk  
831 char characteristics and its tar adsorption capability. *Energies*, **5**(12), 4941-4951.
- 832 **54.** Petrović, J.T., Stojanović, M.D., Milojković, J.V., Petrović, M.S., Šoštarić, T.D.,  
833 Laušević, M.D., Mihajlović, M.L. 2016. Alkali modified hydrochar of grape pomace as a  
834 perspective adsorbent of Pb<sup>2+</sup> from aqueous solution. *Journal of Environmental*  
835 *Management*, **182**, 292-300.
- 836 **55.** Pietrzak, R., Nowicki, P., Kaźmierczak, J., Kuszyńska, I., Goscianska, J., Przepiórski, J.  
837 2014. Comparison of the effects of different chemical activation methods on properties of  
838 carbonaceous adsorbents obtained from cherry stones. *Chemical Engineering Research*  
839 *and Design*, **92**(6), 1187-1191.
- 840 **56.** Qian, K., Kumar, A., Patil, K., Bellmer, D., Wang, D., Yuan, W., Huhnke, R.L. 2013.  
841 Effects of biomass feedstocks and gasification conditions on the physiochemical  
842 properties of char. *Energies*, **6**(8), 3972-3986.
- 843 **57.** Qian, L., Zhang, W., Yan, J., Han, L., Chen, Y., Ouyang, D., Chen, M. 2017. Nanoscale  
844 zero-valent iron supported by biochars produced at different temperatures: Synthesis  
845 mechanism and effect on Cr(VI) removal. *Environmental Pollution*, **223**, 153-160.
- 846 **58.** Rajapaksha, A.U., Chen, S.S., Tsang, D.C., Zhang, M., Vithanage, M., Mandal, S., Gao,  
847 B., Bolan, N.S., Ok, Y.S. 2016. Engineered/designer biochar for contaminant  
848 removal/immobilization from soil and water: potential and implication of biochar  
849 modification. *Chemosphere*, **148**(27), 6e291.
- 850 **59.** Rawal, A., Joseph, S.D., Hook, J.M., Chia, C.H., Munroe, P.R., Donne, S., Lin, Y.,  
851 Phelan, D., Mitchell, D.R., Pace, B. 2016. Mineral–Biochar Composites: Molecular  
852 Structure and Porosity. *Environmental science & technology*, **50**(14), 7706-7714.
- 853 **60.** Ren, J., Li, N., Li, L., An, J.-K., Zhao, L., Ren, N.-Q. 2015. Granulation and ferric oxides  
854 loading enable biochar derived from cotton stalk to remove phosphate from water.  
855 *Bioresource Technology*, **178**, 119-125.
- 856 **61.** Ren, Y., Yan, N., Feng, J., Ma, J., Wen, Q., Li, N., Dong, Q. 2012. Adsorption  
857 mechanism of copper and lead ions onto graphene nanosheet/ $\delta$ -MnO<sub>2</sub>. *Materials*  
858 *Chemistry and Physics*, **136**(2), 538-544.
- 859 **62.** Roy, E.D. 2016. Phosphorus recovery and recycling with ecological engineering: A  
860 review. *Ecological Engineering*, **98**, 213-227.
- 861 **63.** Shang, M.-r., Liu, Y.-g., Liu, S.-b., Zeng, G.-m., Tan, X.-f., Jiang, L.-h., Huang, X.-x.,  
862 Ding, Y., Guo, Y.-m., Wang, S.-f. 2016. A novel graphene oxide coated biochar  
863 composite: synthesis, characterization and application for Cr (VI) removal. *RSC*  
864 *Advances*, **6**(88), 85202-85212.
- 865 **64.** Shannon, M.A., Bohn, P.W., Elimelech, M., Georgiadis, J.G., Marinas, B.J., Mayes,  
866 A.M. 2008. Science and technology for water purification in the coming decades. *Nature*,  
867 **452**(7185), 301-310.

- 868 **65.** Shim, T., Yoo, J., Ryu, C., Park, Y.-K., Jung, J. 2015. Effect of steam activation of  
869 biochar produced from a giant Miscanthus on copper sorption and toxicity. *Bioresource*  
870 *technology*, **197**, 85-90.
- 871 **66.** Sitko, R., Turek, E., Zawisza, B., Malicka, E., Talik, E., Heimann, J., Gagor, A., Feist,  
872 B., Wrzalik, R. 2013. Adsorption of divalent metal ions from aqueous solutions using  
873 graphene oxide. *Dalton Transactions*, **42**(16), 5682-5689.
- 874 **67.** Sizmur, T., Quilliam, R., Puga, A.P., Moreno-Jiménez, E., Beesley, L., Gomez-Eyles,  
875 J.L. 2016. Application of biochar for soil remediation. *Agricultural and Environmental*  
876 *Applications of Biochar: Advances and Barriers*(sssaspepub63), 295-324.
- 877 **68.** Song, Z., Lian, F., Yu, Z., Zhu, L., Xing, B., Qiu, W. 2014. Synthesis and  
878 characterization of a novel MnOx-loaded biochar and its adsorption properties for Cu<sup>2+</sup>  
879 in aqueous solution. *Chemical Engineering Journal*, **242**, 36-42.
- 880 **69.** Soudek, P., Valseca, I.R., Petrová, Š., Song, J., Vaněk, T. 2016. Characteristics of  
881 different types of biochar and effects on the toxicity of heavy metals to germinating  
882 sorghum seeds. *Journal of Geochemical Exploration*.
- 883 **70.** Tan, X., Liu, Y., Zeng, G., Wang, X., Hu, X., Gu, Y., Yang, Z. 2015. Application of  
884 biochar for the removal of pollutants from aqueous solutions. *Chemosphere*, **125**, 70-85.
- 885 **71.** Tang, J., Lv, H., Gong, Y., Huang, Y. 2015. Preparation and characterization of a novel  
886 graphene/biochar composite for aqueous phenanthrene and mercury removal.  
887 *Bioresource technology*, **196**, 355-363.
- 888 **72.** Trakal, L., Veselská, V., Šafařík, I., Vítková, M., Číhalová, S., Komárek, M. 2016. Lead  
889 and cadmium sorption mechanisms on magnetically modified biochars. *Bioresource*  
890 *technology*, **203**, 318-324.
- 891 **73.** Tripathi, M., Sahu, J., Ganesan, P. 2016. Effect of process parameters on production of  
892 biochar from biomass waste through pyrolysis: A review. *Renewable and Sustainable*  
893 *Energy Reviews*, **55**, 467-481.
- 894 **74.** Uchimiya, M., Lima, I.M., Thomas Klasson, K., Chang, S., Wartelle, L.H., Rodgers, J.E.  
895 2010. Immobilization of heavy metal ions (CuII, CdII, NiII, and PbII) by broiler litter-  
896 derived biochars in water and soil. *Journal of Agricultural and Food Chemistry*, **58**(9),  
897 5538-5544.
- 898 **75.** Vu, T.M., Doan, D.P., Van, H.T., Nguyen, T.V., Vigneswaran, S., Ngo, H.H. 2017.  
899 Removing ammonium from water using modified corncob-biochar. *Science of The Total*  
900 *Environment*, **579**, 612-619.
- 901 **76.** Wang, H., Tian, Z., Jiang, L., Luo, W., Wei, Z., Li, S., Cui, J., Wei, W. 2017a. Highly  
902 efficient adsorption of Cr (VI) from aqueous solution by Fe<sup>3+</sup> impregnated biochar.  
903 *Journal of Dispersion Science and Technology*, **38**(6), 815-825.
- 904 **77.** Wang, S.-y., Tang, Y.-k., Li, K., Mo, Y.-y., Li, H.-f., Gu, Z.-q. 2014. Combined  
905 performance of biochar sorption and magnetic separation processes for treatment of  
906 chromium-contained electroplating wastewater. *Bioresource technology*, **174**, 67-73.
- 907 **78.** Wang, S., Gao, B., Li, Y. 2016. Enhanced arsenic removal by biochar modified with  
908 nickel (Ni) and manganese (Mn) oxyhydroxides. *Journal of Industrial and Engineering*  
909 *Chemistry*, **37**, 361-365.

- 910 **79.** Wang, S., Gao, B., Li, Y., Creamer, A.E., He, F. 2017b. Adsorptive removal of arsenate  
911 from aqueous solutions by biochar supported zero-valent iron nanocomposite: Batch and  
912 continuous flow tests. *Journal of hazardous materials*, **322**, 172-181.
- 913 **80.** Wang, S., Gao, B., Li, Y., Mosa, A., Zimmerman, A.R., Ma, L.Q., Harris, W.G.,  
914 Migliaccio, K.W. 2015a. Manganese oxide-modified biochars: Preparation,  
915 characterization, and sorption of arsenate and lead. *Bioresource technology*, **181**, 13-17.
- 916 **81.** Wang, S., Gao, B., Zimmerman, A.R., Li, Y., Ma, L., Harris, W.G., Migliaccio, K.W.  
917 2015b. Removal of arsenic by magnetic biochar prepared from pinewood and natural  
918 hematite. *Bioresource technology*, **175**, 391-395.
- 919 **82.** Xu, X., Cao, X., Zhao, L. 2013. Comparison of rice husk- and dairy manure-derived  
920 biochars for simultaneously removing heavy metals from aqueous solutions: Role of  
921 mineral components in biochars. *Chemosphere*, **92**(8), 955-961.
- 922 **83.** Xue, Y., Gao, B., Yao, Y., Inyang, M., Zhang, M., Zimmerman, A.R., Ro, K.S. 2012.  
923 Hydrogen peroxide modification enhances the ability of biochar (hydrochar) produced  
924 from hydrothermal carbonization of peanut hull to remove aqueous heavy metals: Batch  
925 and column tests. *Chemical Engineering Journal*, **200–202**, 673-680.
- 926 **84.** Yang, G.-X., Jiang, H. 2014. Amino modification of biochar for enhanced adsorption of  
927 copper ions from synthetic wastewater. *water research*, **48**, 396-405.
- 928 **85.** Yao, Y., Gao, B., Chen, J., Zhang, M., Inyang, M., Li, Y., Alva, A., Yang, L. 2013.  
929 Engineered carbon (biochar) prepared by direct pyrolysis of Mg-accumulated tomato  
930 tissues: characterization and phosphate removal potential. *Bioresource technology*, **138**,  
931 8-13.
- 932 **86.** Yao, Y., Gao, B., Fang, J., Zhang, M., Chen, H., Zhou, Y., Creamer, A.E., Sun, Y.,  
933 Yang, L. 2014. Characterization and environmental applications of clay–biochar  
934 composites. *Chemical Engineering Journal*, **242**, 136-143.
- 935 **87.** Yu, P., Xue, Y., Gao, F., Liu, Z., Cheng, X., Yang, K. 2016. Phosphorus Removal from  
936 Aqueous Solution by Pre-or Post-Modified Biochars Derived from Agricultural  
937 Residues. *Water, Air, & Soil Pollution*, **227**(10), 370.
- 938 **88.** Yuan, J.-H., Xu, R.-K., Zhang, H. 2011. The forms of alkalis in the biochar produced  
939 from crop residues at different temperatures. *Bioresource technology*, **102**(3), 3488-3497.
- 940 **89.** Zhang, F., Wang, X., Xionghui, J., Ma, L. 2016. Efficient arsenate removal by magnetite-  
941 modified water hyacinth biochar. *Environmental Pollution*, **216**, 575-583.
- 942 **90.** Zhang, M.-m., Liu, Y.-g., Li, T.-t., Xu, W.-h., Zheng, B.-h., Tan, X.-f., Wang, H., Guo,  
943 Y.-m., Guo, F.-y., Wang, S.-f. 2015. Chitosan modification of magnetic biochar  
944 produced from *Eichhornia crassipes* for enhanced sorption of Cr (vi) from aqueous  
945 solution. *RSC Advances*, **5**(58), 46955-46964.
- 946 **91.** Zhang, M., Gao, B. 2013. Removal of arsenic, methylene blue, and phosphate by  
947 biochar/AlOOH nanocomposite. *Chemical Engineering Journal*, **226**, 286-292.
- 948 **92.** Zhang, M., Gao, B., Varnosfaderani, S., Hebard, A., Yao, Y., Inyang, M. 2013a.  
949 Preparation and characterization of a novel magnetic biochar for arsenic removal.  
950 *Bioresource technology*, **130**, 457-462.



- 951 **93.** Zhang, M., Gao, B., Yao, Y., Inyang, M. 2013b. Phosphate removal ability of  
952 biochar/MgAl-LDH ultra-fine composites prepared by liquid-phase deposition.  
953 *Chemosphere*, **92**(8), 1042-1047.
- 954 **94.** Zhang, M., Gao, B., Yao, Y., Xue, Y., Inyang, M. 2012. Synthesis of porous MgO-  
955 biochar nanocomposites for removal of phosphate and nitrate from aqueous solutions.  
956 *Chemical Engineering Journal*, **210**, 26-32.
- 957 **95.** Zhao, G., Li, J., Ren, X., Chen, C., Wang, X. 2011. Few-layered graphene oxide  
958 nanosheets as superior sorbents for heavy metal ion pollution management.  
959 *Environmental science & technology*, **45**(24), 10454-10462.
- 960 **96.** Zhao, L., Zheng, W., Mašek, O., Chen, X., Gu, B., Sharma, B.K., Cao, X. 2017. Roles of  
961 Phosphoric Acid in Biochar Formation: Synchronously Improving Carbon Retention and  
962 Sorption Capacity. *Journal of Environmental Quality*, **46**(2), 393-401.
- 963 **97.** Zhou, L., Huang, Y., Qiu, W., Sun, Z., Liu, Z., Song, Z. 2017a. Adsorption Properties of  
964 Nano-MnO<sub>2</sub>-Biochar Composites for Copper in Aqueous Solution. *Molecules*, **22**(1),  
965 173.
- 966 **98.** Zhou, Y., Gao, B., Zimmerman, A.R., Chen, H., Zhang, M., Cao, X. 2014. Biochar-  
967 supported zerovalent iron for removal of various contaminants from aqueous solutions.  
968 *Bioresource technology*, **152**, 538-542.
- 969 **99.** Zhou, Y., Gao, B., Zimmerman, A.R., Fang, J., Sun, Y., Cao, X. 2013. Sorption of heavy  
970 metals on chitosan-modified biochars and its biological effects. *Chemical Engineering*  
971 *Journal*, **231**, 512-518.
- 972 **100.** Zhou, Z., Liu, Y.-g., Liu, S.-b., Liu, H.-y., Zeng, G.-m., Tan, X.-f., Yang, C.-p., Ding, Y.,  
973 Yan, Z.-l., Cai, X.-x. 2017b. Sorption performance and mechanisms of arsenic (V)  
974 removal by magnetic gelatin-modified biochar. *Chemical Engineering Journal*, **314**, 223-  
975 231.
- 976
- 977
- 978